STUDIES OF THE SUPERNUMERARY SUBUNIT OF CYTOCHROME bc_1 COMPLEX FROM *RHODOBACTER SPHAEROIDES*

By

SHIH-CHIA TSO

Bachelor of Science
National Taiwan University
Taipei, Taiwan
1988

Master of Science
Oklahoma State University
Stillwater, Oklahoma
1995

Submitted to the Faculty of the
Graduate College of the
Oklahoma State University
in partial fulfillment of
the requirements for
the Degree of
DOCTOR OF PHILOSOPHY
July, 2004

STUDIES OF THE SUPERNUMERARY SUBUNIT OF

CYTOCHROME bc_1 COMPLEX FROM

RHODOBACTER SPHAEROIDES

Thesis Approved:

Linda Yu

Thesis Adviser

Chang-An Yu

Richard Essenberg

Jose Soulages

Robert Burnap

Al Carlozzi

Dean of the Graduate College

ACKNOWLEDGEMENTS

I wish to express my sincere appreciation to my advisor, Dr. Linda Yu for her intelligent supervision, constructive guidance, inspiration and friendship. My sincere appreciation extends to my other committee members Dr. Chang-An Yu, Dr. Richard Essenberg, Dr. Jose Soulages, and Dr. Robert Burnap, whose guidance, assistance, encouragement, and friendship are also invaluable. More over, I wish to express my sincere gratitude to those who provided suggestions and assistance for this study: Dr. Michael Mather, Dr. Yeong-Renn Chen, Dr. Sudha Shenoy, Dr. Hua Tian, Dr. Di Xia (NIH), Mr. Byron Quinn, and all my friends in the lab. I also thank Mr. Buddha Gurung and Ms. Maria Eberry for proofreading this dissertation.

Finally, I would like to give my special appreciation to my parents, parents in law and my wife Shuyi Chang for their support and encouragement.

TABLE OF CONTENTS

LIST OF TABLES

LIST OF FIGURES

ABBREVIATIONS

ADP	adenosine diphosphate
ATP	adenosine triphosphate
BSA	bovine serum albumin
cyt	cytochrome
CD	circular dichroism
dam	DNA adenine methylation
DM	dodecyl β-maltoside
DMSO	dimethyl sulfoxide
DSC	differential scanning calorimetry
ε	extinction coefficient
E. coli	*Escherichia coli*
FPLC	fast protein liquid chromatography
GST	glutathione S-transferase
ICM	intra-cytoplasmic membrane
IPTG	isopropyl β-D-thiogalactopyranoside
ISP	Rieske iron-sulfur protein
kDa	kilodaltons
kb	kilo base pair

LB	Lennox L. Broth
MCLA	2-methyl-6-(-*p*-methoxyphenyl)-3,7-ddihydroimidazo[1,2-α]pyrazin-3-one hydrochloride; or methyl *Cypridina* luciferin analog
NAD	nicotinamide adenine dinucleotide, oxidized form
NADH	nicotinamide adenine dinucleotide, reduced form
NADP	nicotinamide adenine dinucleotide phosphate, oxidized form
NADPH	nicotinamide adenine dinucleotide phosphate, reduced form
PAGE	polyacrylamide gel electrophoresis
PBS	phosphate buffered saline
PC	plastocyanin
PCR	polymerase chain reaction
PMSF	phenylmethylsulfonyl fluoride
ppt	precipitate
PQ	plastoquinol
psi	pound per square inch
Q	ubiquinone
QH_2	ubiquinol
QCR	ubiquinol-cytochrome *c* reductase
rpm	revolutions per minute
R. sphaeroides	*Rhodobacter sphaeroides*
SDS	sodium dodecyl sulfate
Tris	Tris(hydroxymethyl)aminomethane

UHDBT	5-n-undecyl-6-hydroxy-4,7-dioxobenzothiazole

CHAPTER I

INTRODUCTION

Cytochrome bc_1 Complex in Respiration and Photosynthesis

The cytochrome bc_1 complex, or ubiquinol-cytochrome *c* oxidoreductase, which can be found in the inner membrane of mitochondria or in cytoplasmic membrane of many bacteria, is a central component of the electron transfer pathway for their respiration or photosynthesis (1-5). The complex catalyzes the oxidation of quinol and reduction of soluble *c*-type cytochromes with the generation of a proton gradient and a membrane potential. The combination of the proton gradient and the membrane potential is referred to as proton motive force (pmf). The pmf is the driving force for synthesis of ATP by the F_1F_0-ATP synthase in the membrane.

All the cytochrome bc_1 complexes contain four redox centers: two *b* type hemes (b_H and b_L) in a cytochrome *b* subunit, one *c* type heme (c_1) in a cytochrome c_1 subunit, and a high potential [2Fe-2S] cluster in the Rieske iron-sulfur protein.

In chloroplasts and cyanobacteria, a very similar complex called the cytochrome b_6f complex, or plastoquinol-plastocyanin oxidoreductase, replaces the cytochrome bc_1 complex for participation in the electron transfer chains of their oxygen-evolving

photosynthesis. The cytochrome b_6f complex has a smaller cytochrome *b* subunit corresponding to only the N-terminal heme-bearing part of bc_1 complex's cytochrome *b* subunit, while a sequence similar to the C-terminal part is present in a separate subunit (6,7). The cytochrome *f* is structurally unrelated to cytochrome c_1, although the cytochrome *f* is a c-type cytochrome. Because of the similarity between bc_1 and b_6f, the term "cytochrome bc_1 complex" is often used to include the cytochrome b_6f complex (3), and most features of bc_1 complex discussed here should apply to the b_6f complex as well.

The cytochrome bc_1 complex does not exist universally in all organisms (3). For example, some bacteria like *Escherichia coli* do not possess a bc_1 complex, and they complete their respiration by transferring electrons directly from ubiquinol to oxygen via an ubiquinol-oxidase, cytochrome bo_3. However, since the cytochrome bc_1 complex is a central component of the electron-transfer pathway for both mitochondria and chloroplast, it is an absolutely necessity for eukaryotic organisms.

In mitochondria, the cytochrome bc_1 complex, usually known as complex III, is a part of the respiratory electron-transport chain. Two products of the citric acid cycle, NADH and succinate, are electron donors of the electron-transport chain. Electrons are passed from NADH through complex I (NADH-ubiquinone reductase), or from succinate through complex II (succinate-ubiquinone reductase), and then to ubiquinone, complex III, cytochrome *c*, complex IV (cytochrome *c* oxidase), and to a final electron acceptor—oxygen. Protons are translocated across the membrane as electrons pass through these complexes (except complex II) to generate the proton motive force as mentioned above. In the aerobic respiratory system of bacteria, the bc_1 complex plays a similar role as the one in mitochondria.

In addition to the respiratory system, the bc_1 complex is also found in bacterial photosynthetic electron transport systems. In the facultative photosynthetic purple non-sulfur bacterium *Rhodobacter sphaeroides*, there is a cyclic photosynthetic pathway with the bc_1 complex as an obligatory electron transfer complex. The photosynthetic electron transfer is initiated as the light energy is absorbed inside the photosynthetic reaction center by the primary donor, P_{870} (a bacteriochlorophyll), which has an absorption maximum at 870 nm. Light-harvesting complexes surrounding the reaction center help absorb the light more effectively over a wide range of wavelengths shorter than 870 nm. The light-harvesting complexes are proteins attached with bacteriochlorophyll and carotenoid pigments. Excited by the light energy, the P_{870} becomes a relatively stronger reducing agent (lower redox potential), and is thermodynamically capable of donating an electron to the next electron carrier. The electron is then transferred inside the reaction center to a bound quinone at site Q_B via a second bacteriochlorophyll, a bacteriopheophytin, and a bound quinone at site Q_A. After accepting two electrons, the quinone at the site Q_B becomes fully reduced as Q^{2-}, and immediately uptakes two protons from the cytoplasm (negative side) to produce QH_2. The reduced QH_2 can now serve as the substrate for the ubiquinol-cytochrome *c* reductase reaction in the bc_1 complex.

Same as in the mitochondrial bc_1 complex, for every mole of QH_2 that is oxidized, two moles of cytochrome c_2 (cytochrome *c* equivalent in purple bacteria) are reduced, and four moles of proton are translocated across the membrane. The reduced cytochromes c_2 then carry electrons back to the photosynthetic reaction center and reduce the P_{870} of the reaction center. Therefore, in this cyclic pathway, there is no exogenous electron donor

or a final electron acceptor. Electrons continuously recycled between the reaction center and the bc_1 complex with light energy serving as the driving force, resulting protons pumped across the membrane to form the proton motive force.

A more complicated photosynthetic pathway occurs in chloroplast with cytochrome b_6f complexes instead of cytochrome bc_1 complexes. However, as mentioned above, cytochrome b_6f complex is very similar to cytochrome bc_1 complex structurally and functionally. There are two photosynthetic reaction centers in this pathway, photosystem I and photosystem II. The photosystem II is equivalent to the reaction center in *R. sphaeroides*, but there is no cyclic pathway between photosystem II and cytochrome b_6f complex as in *R. sphaeroides*. In chloroplast, water is the electron donor for the photosysthesis, and electrons are released from a water splitting reaction, which is absent in the bacterial reaction center. Plastoquinol (PQ, and equivalent of ubiquinol), which is reduced in photosystem II, transfers electrons through the cytochrome b_6f complex to plastocyanin (PC, an equivalent of cytochrome *c*). The reduced PC then transfers its electron to photosystem I. Excited by light energy, photosystem I transfers the electrons to $NADP^+$ and produce NADPH via an NADP reductase. The major difference between photosystem I and II is that the redox potential of photosystem I is low enough to reduce $NADP^+$. Therefore, in addition to the generated proton motive force, a strong electron donor (NADPH) is produced by this pathway. An alternative cyclic photosynthetic pathway also exists in chloroplasts: the electrons from excited photosystem I can go back to cytochrome b_6f complex via the plastoquinone. In this case, more proton motive force is generated by the cytochrome b_6f complex for ATP synthesis without the need for synthesizing any NADPH.

Q-Cycle Mechanism

The bc_1 complex can basically be considered as a "proton pump" which moves protons across the membrane by utilizing the potential energy due to the redox potential difference between ubiquinol and cytochrome *c*. The simplest arrangement for electron transfer should be a linear pathway, in where, the electron transfer components are arranged in an ascending order of their redox potentials as shown here:

$$QH_2 \longrightarrow b_L \longrightarrow b_H \longrightarrow ISP \longrightarrow c_1 \longrightarrow c$$

The immediate problem of this model is the difficulty in explaining the two-protons/one-electron stoichiometry of the reaction observed in the bc_1 complex (8). Among all the electron transfer components within the bc_1 complex, only ubiquinol serves as a carrier for both protons and electrons. Therefore, for every electron going through the complex, only one proton has the chance to be translocated in the linear electron transfer model.

In addition, the linear model is very unlikely to be the electron transfer pathway because it can not explain the phenomenon known as "oxidant-induced reduction of cytochrome *b*". This phenomenon was observed by Chance (9): addition of a pulse of oxygen to slowly respiring mitochondria causes a transient increased reduction of the cytochrome *b*, particularly in the presence of the inhibitor antimycin. If the linear model were true, we would expect to observe increased oxidation of cytochrome c_1, ISP, cytochrome *b* and ubiquinol following a sudden increase of oxidation of cytochrome *c*.

Therefore, a more complicated model known as the "Q cycle mechanism" (see Fig. 1) was first proposed by Mitchell (10) and modified later (8,11,12) to explain the electron

transfer, the proton translocation, the 2:1 H^+/e^- ratio and the "oxidant-induced reduction of cytochrome *b*" in the cytochrome bc_1 complex. Although there are still some different opinions (13,14), it is generally accepted that bc_1 complexes operate through the "Q cycle mechanism".

The two key features of the Q cycle mechanism are 1) the presence of two separate ubiquinone binding sites: Q_o site and Q_i site, and 2) the bifurcated reaction at the Q_o site (8). In the bifurcated reaction at the Q_o site, one of the two electrons from ubiquinol oxidation is "recycled" through cytochrome *b*, and the ubiquinol can be used one more time to carry two more protons. Therefore it takes only two electrons to translocate four protons across the membrane. Although the detailed mechanism of the bifurcation of quinol oxidation at the Q_o site is still controversial, it is believed that an ubiquinol (QH_2) at the Q_o site is oxidized by ISP and cytochrome b_L in either a concerted mechanism (15-17) or a sequential mechanism (18-20). In the concerted mechanism, an electron is transferred to heme b_L as soon as the other electron is transferred to ISP, and therefore no semiquinone is generated (see Fig. 1-A). In the sequential mechanism, the heme b_L is reduced by an intermediate ubisemiquinone generated at the Q_o site after the first electron is transferred to ISP (see Fig. 1-B). However, the presence of such semiquinone has not been detected (16,21).

In both mechanisms, two protons are released into the positive side of the membrane when the quinol is oxidized. The electron, which has been transferred to ISP, is then transferred to cytochrome c_1 and then to cytochrome *c*. The other electron, which is transferred to the b_L heme, is then moved to the b_H heme. At the Q_i site, a ubiquinone (Q_i) accepts an electron from the b_H heme to form a relatively stable ubisemiquinone ($\cdot Q_i^-$

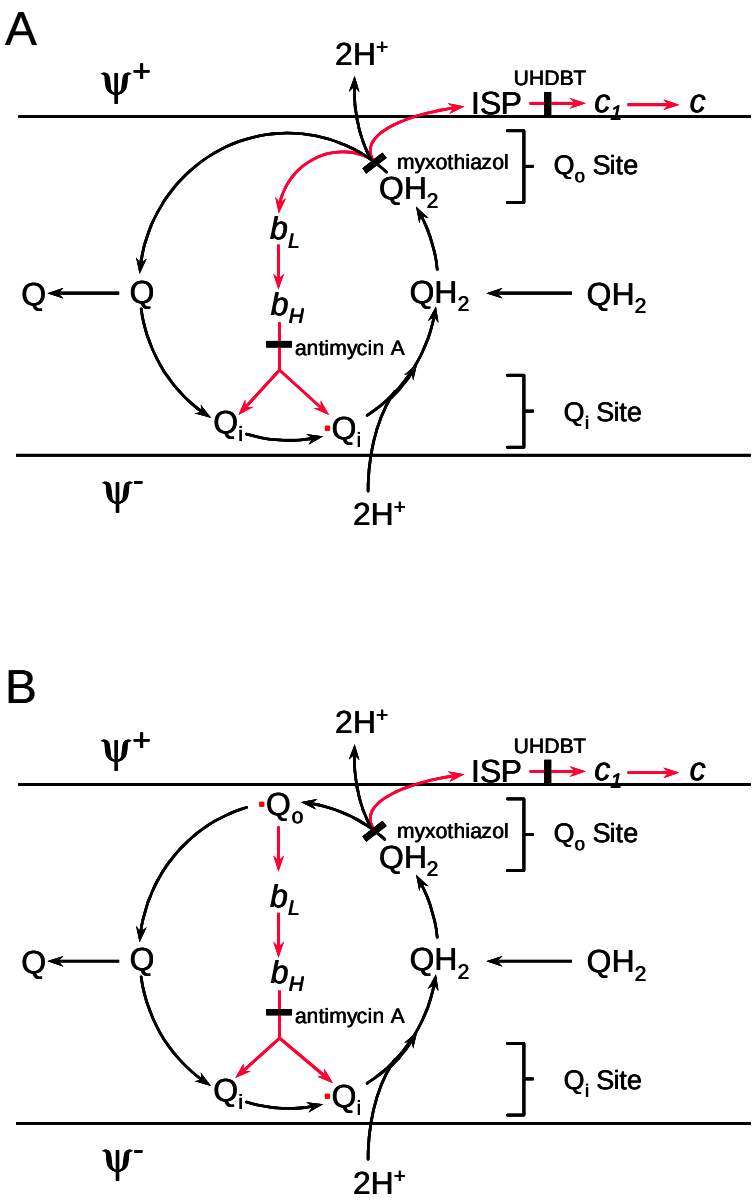

FIG. 1. **The Q-cycle with (A) Concerted and (B) Sequential Bifurcated Reaction at Qo Site.** Red lines indicate the electron transfer between redox centers. The black bars show the sites, at which inhibits block electron transfer within the complex.

). At this point, the reaction is only half complete, with only one of two electrons from ubiquinol being transferred to cytochrome *c*.

In the second half of the Q cycle, all steps are repeated: one ubiquinol is oxidized, one cytochrome *c* is reduced, two protons are deposited into the positive side of the membrane, and the b_H heme is reduced via the b_L heme. At the Q_i site, the ubisemiquinone, which is generated in the first half of the Q cycle, accepts another electron from the b_H heme and uptakes two protons from the negative side of the membrane to form ubiquinol (QH_2) and complete one Q cycle. The net result of one complete Q cycle generates one molecule of oxidized ubiquinone, two molecules of reduced cytochrome *c*, uptake two protons from the negative side of the membrane, and deposits four protons to the positive side of the membrane,

$$QH_2 + 2 \text{ cyt } c^{3+} + 2H^+_{(\text{N-side})} \rightarrow Q + 2 \text{ cyt } c^{2+} + 4H^+_{(\text{P-side})}.$$

Three-Dimensional Crystal Structures of Cytochrome bc_1 and b_6f Complex

Three-dimensional structures of mitochondrial bc_1 complexes from bovine (22,23) and chicken (24) were determined by crystallization and x-ray diffraction at about 3 Å resolutions by three groups initially, and later the resolutions were improved to 2.3 Å in the yeast bc_1 (25), and 2.4 Å in the bovine bc_1 structure (26). The structure of the bovine mitochondrial bc_1 complex is dimeric and pear-shaped. The height of the complex is approximately 155 Å, and its diameter at its widest point in the matrix space is about 130 Å. The complex extends 38 Å into the cytoplasmic space, spans the 42 Å inner mitochondrial membrane, and projects 75 Å into the matrix space. The subunits core 1

and core 2, along with subunits 6 and 9, lie entirely in the matrix space. Cytochrome *b*, cytochrome c_1, ISP, and subunits 7, 10, and 11 span the membrane, whereas subunit 8 lies solely on the intermembrane space.

Recently, the crystal structures of cytochrome b_6f complexes from the cyanobacteria (blue-green algae) *Mastigocladus laminosus* (27) and *Chlamydomonas reinhardtti* (28) were also solved at 3.0 Å and 3.1 Å respectively. The crystal structure of b_6f complex shows also a dimer whose core organization is similar to that of bc_1 complex (27,28). Although cytochromes *f* and c_1 are not homologous, they occupy roughly equivalent positions in the two complexes. However, the domain arrangement outside the core of the b_6f complex is different from bc_1 complex due to the position of those small subunits PetF, PetL, PetM and PetN. Most striking difference between bc_1 and b_6f is that an additional heme, which is located close to the heme b_H, is found in the structure of b_6f complex.

With 2.3 Å resolution of the structure, many questions about the detailed mechanism still remain unanswered, so a structure with better resolution is still needed. However, the current x-ray structure supports the Q-cycle mechanism, but also suggests two unexpected features of the complex. The most dramatic one is the mobile nature of the head domain of the ISP during bc_1 catalysis. The second one is that the dimeric structure may be essential for proper function of the cytochrome bc_1 complex.

Movement of Head Domain of ISP

The mobility of the ISP during bc_1 catalysis was first suggested by the observation of the low electron density of its extramembrane head domain (22). The mobile hypothesis is further supported by observations of the different positions of the [2Fe-2S] cluster in

the presence of various Q_o site inhibitors (23,24,29). To study the movement of the ISP head domain by using mutagenesis in *R. sphaeroides* bc_1, Tian *et al*. (30) demonstrated that increasing the rigidity of the ISP neck region by a double-proline substitution at Ala-46 and Ala-48 or a triple-proline substitution at residues 42-44 decreased the activity and increased the activation energy. In a continuous work, Tian *et al*.(31) constructed mutants with cysteines pairs in the ISP neck region; oxidation of the cystines pair to form a disulfide bond to restrict the flexibility of the ISP neck region decreases activity, which can be restored by reducing the disulfide bond with β-mercaptoethanol. To further establish the essentiality of the movement of the head domain of ISP, *R. sphaeroides* bc_1 mutant with a pair of cysteines between cytochrome *b* and the head domain of ISP was generated (32); formation of the inter-subunit disulfide bond, which immobilizes the ISP head at the b position, is concurrent with the loss of its bc_1 activity, and reduction of this disulfide bond by β-mercaptoethanol restores the activity.

The hypothesis of the mobility of the ISP head domain not only provides an explanation for the unexpected findings in those crystal structures, but it may also provide an explaination for the bifurcated reaction at Qo site. The bifurcated quinol oxidation at the Q_o site is the key step in the Q cycle mechanism as mentioned in the previous section. The major problem for the obligatory bifurcated reaction is that one of the two electrons from quinol has to be transferred to the unfavorable low potential chain (cytochrome b_L and b_H). It is difficult to explain why both electrons are not moved to the thermodynamically favorable high potential chain (ISP and cytochrome c_1). Several models are proposed trying to explain how the bifurcated reaction is controlled, such as the catalytic switch model (33), the proton-gate affinity change model (15), and the

double-occupancy Qo site model (34). However, the observation of the mobility of the ISP head domain provides a new insight into the bifurcation reaction mechanism. In the structure-based model, it is suggested that the reduced ISP head is held in the position close to cytochrome *b* (b-position) until the second electron is transferred to the low potential chain triggering the movement of the ISP head to the position close to cytochrome c_1 (c position) (29,35). Since the reduced ISP head in the "b-position" is too far away from cytochrome c_1 to rapidly transfer electron to cytochrome c_1, the ISP would keep its reduced state and the second electron of the quinol is not able to go to ISP but to cytochrome *b* (36). Another possible model based on the structure suggests that the reoxidized ISP is unable to return to the b-position to be re-reduced, before the second electron is transferred to the low potential chain (20).

The Intertwined Dimeric Structure of Cytochrome bc_1 Complex

Several observations in the crystal structure suggest that the cytochrome bc_1 complex is functioning as a dimer (22); 1) the distance between two b_L hemes in the two monomers is short enough (21 Å) to transfer electrons between them; 2) the extrinsic domain of the iron-sulfur protein of one monomer is in a position close to cytochrome *b* and cytochrome c_1 of the other monomer; i.e. the trans-membrane helix of an iron-sulfur protein is on one monomer while the extrinsic domain is on the other monomer; 3) there is an internal cavity in the complex that connects the Q_o pocket of one monomer to the Q_i pocket of the other.

To confirm that the cytochrome bc_1 complex exists as a dimer with intertwining Rieske iron-sulfur proteins not only in crystal but also in solution, Xiao *et al.* (37) demonstrated that the cytochrome bc_1 complex exists as a dimer with intertwining Rieske

ISPs by using a *R. sphaeroides* bc_1 mutant containing two cysteines pairs. One pair was in the interface between the head domain of ISP and cytochrome *b*, and the other was between the tail domain of ISP and cytochrome *b*. An adduct protein with an apparent molecular mass of 128 kDa containing two cytochrome *b* and two ISP proteins is detected on SDS-PAGE as the protein samples were not treated by β-mercaptoethanol, confirming that the bc_1 complex exists as a dimer with intertwining ISPs.

Recently, Gutierrez-Cirlos and Trumpower (38) demonstrated that in the yeast bc_1 complex, stigmatellin and methoxyacrylate stilbene inhibit the enzyme activity with a stoichiometry of 0.5 per complex. The results indicate that only one molecule of such an inhibitor is sufficient to completely inhibit two molecules of the bc_1 complex and suggest the essentiality of the dimeric structure for bc_1's function.

An ongoing experiment in our lab showing that there may be electron transfer between two monomer of the complex (unpublished result), also implies the functional significance of the dimeric structure of the complex.

Supernumerary Subunits of Cytochrome bc_1 Complex

The protein subunits in the cytochrome bc_1 complex can be divided into two groups: those that contain a redox prosthetic group, called the core subunits, and those that do not, called the supernumerary subunits (39). All cytochrome bc_1 complexes contain three core subunits: cytochrome *b*, cytochrome c_1 and Rieske ISP, but they vary significantly in the supernumerary subunit composition. For example, the bc_1 complex from bovine heart mitochondria has eight supernumerary subunits (40); that from yeast (41) has seven; that

of *R. sphaeroides* has one (42), whereas the complexes from *Rhodopseudomonas rubrum* (43), *Paracoccus* denitrificans (39), and *Rhodobacter capsulatus* (44) have none. Although the functions of supernumerary subunit are not fully understood, the complexes containing no supernumerary subunit are less stable and have lower activity than those with supernumerary subunits (41). It has been reported that cytochrome bc_1 complexes purified from the mitochondria of bovine heart and yeast, and from the chromatophores of *R. spharoides* and *R. capsulatus* by a single chromatographic procedure have the turnover rates of 1152, 219, 128, and 64 s^{-1}, respectively (41). The increased activity in mitochondrial and *R. sphaeroides* complexes may result from interactions of the core subunits with supernumerary subunits.

Despite the extensive studies of the three redox-group-containing subunits have obtained wealth of knowledge, the functions of the supernumerary subunits are largely unknown. Some studies have been conducted on the function of the supernumerary subunits, most of them using the mitochondrial cytochrome bc_1 complex. Subunit I and II of yeast bc_1 are suggested to be essential for maintaining the proper conformation of apocytochrome *b* to aid in the addition of heme (45,46); subunit VI of yeast bc_1 is involved in manipulating dimer/monomer transition (47,48); subunit VII and VIII of yeast bc_1 are essential for assembly of the complex (49); subunit IX of yeast bc_1 interacts with the iron-sulfur protein, cytochrome *b* and cytochrome c_1 (50); subunit I and II of plant or bovine bc_1 have the mitochondrial-processing peptidase activity (51,52). However, the presence of multiple supernumerary subunits in the mitochondrial cytochrome bc_1 complexes makes their studies complicated. The cytochrome bc_1 complex from *R.*

sphaeroides, with only one supernumerary subunit, is therefore an ideal system to study the function of the supernumerary subunits.

Photosynthetic Bacteria *Rhodobacter sphaeroides*

Rhodobacter sphaeroides is an anoxygenic, non-sulfur, purple facultative photosynthetic bacterium. In contrast to plants and algae, which carry out photosynthesis in an aerobic environment and produce oxygen as a product of the water splitting reaction, *R. sphaeroides* carries out photosynthesis in an anaerobic condition, and does not produce oxygen. Actually, the synthesis of some photosynthetic pigments (e.g. bacteriochlorophyll) in *R. sphaeroides* is repressed by oxygen (53). Its preferred growth mode is photoheterotrophic, under anaerobic conditions in light with various organic substrates. Therefore, the ecological niches of *R. sphaeroides* are anoxic parts of waters and sediments, which receive light of sufficient quantity and quality to allow phototrophic development (53). However, *R. sphaeroides* is not a strict anaerobe. It is quite tolerant of oxygen and grows well under aerobic conditions in the dark. Under aerobic conditions, synthesis of bacteriochlorophyll is repressed, so the culture becomes pink colored rather than brownish green as seen in photosynthetic cultures.

A very important feature and advantage of *R. sphaeroides* as a material for bc_1 complex study is that the bc_1 complex is not essential for its aerobic growth, since the electron from quinol can be transferred to oxygen via a quinol oxidase as an alternative electron transfer pathway. Therefore, *R. sphaeroides* mutants with severely defective bc_1 complexes are still able to survive and grow in large quantities under aerobic conditions.

However, for preparation of bc_1 complex, the bacteria are grown under "semi-aerobic" conditions in order to have intra-cytoplasmic membrane (ICM) developed inside the bacteria in the presence of limited oxygen.

In addition, bacteria are much easier to handle experimentally than animals, plants and even unicellular eukaryote like yeast, especially for mutagenesis studies. Since the cytochrome bc_1 complex from *R. sphaeroides* is believed similar in its structure and function to the much more complicated complex from mitochondria (4), the mutagenesis results from the bacteria can be applied on the mitochondrial complex. Furthermore, efficient molecular engineering procedures for *R. sphaeroides* are well established, and the genes of all its four subunits have been cloned and sequenced (54,55).

The most important feature that makes the *R. sphaeroides* an ideal system to study the supernumerary subunit of the bc_1 complexes is that it has only one supernumerary subunit -- subunit IV, in contrast to 8 for bovine bc_1 complex, or 7 for yeast bc_1 complex.

Previous Studies on Subunit IV of *Rhodobacter sphaeroides* bc_1 Complex

The *Rhodobacter sphaeroides* cytochrome bc_1 complex was purified from several laboratories with different procedures, and was found to contain four subunits (41,56-58). Subunit IV was found to be an integral part of the complex as follows by using anti-subunit IV affinity column chromatography (59). When detergent-solubilized chromatophore was passed through an anti-subunit IV affinity column, no QCR activity was completely removed in the effluent. Under the identical conditions, when solubilized chromatophore was passed through a preimmune IgG affinity column, only less than 10%

of the activity was lost. When the proteins absorbed to the subunit IV affinity column were eluted with low pH buffer and subjected to SDS-PAGE, all the four subunits of the complex were detected. None of these proteins were found in the eluates of the preimmune IgG affinity column. These results clearly indicate that subunit IV is an integral part of *R. sphaeroides* bc_1 complex.

The gene for subunit IV (*fbcQ*) has been cloned and sequenced (55). Although subunit IV is an integral part of the complex, the *fbc*Q gene is found (55) at least 3 kb away from the *fbc* operon, which encodes ISP (*fbc*F), cytochrome *b* (*fbc*B) and cytochrome c_1 (*fbc*C). The subunit IV gene is 372 base pairs long and encodes 124 amino acid residues. The molecular mass of subunit IV, deduced from the nucleotide sequence, is 14,384 Da. No homology has been found by comparing its sequence with the supernumerary subunits of bc_1 complexes from other organisms. Based on the hydropathy analysis, residues 86 to 109 are predicted as a transmembrane helix (55). The C-terminal end of subunit IV has been suggested to be on the periplasmic side (positive side) and the N-terminal end on the cytoplasmic side (negative side) (60), and this is confirmed in this study.

To facilitate the study of subunit IV, a *fbcQ* gene lacking *R. sphaeroides* strain (RSΔIV) was constructed and characterized (61). There are three characteristic features in this RSΔIV strain, on comparison with the wild-type *R. sphaeroides*: 1) RSΔIV requires a period of adaptation (about 48 hours) before the start of photosynthetic growth; 2) the chemical composition, spectral properties, and the bc_1 activity in chromatophores from the adapted RSΔIV is comparable to wild-typed chromatophores. However, the apparent K_m for Q_2H_2 for the bc_1 reaction in RSΔIV chromatophores is about four times

higher than the wild-type chromatophores; 3) the bc_1 activity in RSΔIV chromatophores is more sensitive to detergent treatment than wild-type chromatophores. These observations suggest the structural role and the Q-binding function of subunit IV (61).

The Q-binding function of subunit IV is supported by photoaffinity labeling using azido-Q derivatives. Analysis of the radioactivity distribution among the subunits of the bc_1 photoaffinity labeled with radioactive azido-Q derivatives shows both cytochrome *b* and subunit IV to be heavily labeled, and hence can be identified as Q-binding proteins (62). To identify the Q-binding domain in subunit IV, a [^{3}H]-azido-Q-labeled subunit IV was isolated and digested by protease V8. The labeled peptide was then separated by HPLC, and identified as amino acid residues 77-124 of subunit IV by sequencing its partial N-terminal (55).

With a similar approach, subunit VII of bovine mitochondrial bc_1 complex was also identified as the small molecular weight Q-binding protein, in addition to cytochrome *b* (63). Based on amino acid sequence comparisons, subunit IV of *R. sphaeroides* bc_1 complex is not homologous with any supernumerary subunits in mitochondrial bc_1 complex, but is functionally homologous to the subunit VII (62,63). Therefore, the subunit IV portion in a proposed 3-D *R. sphaeroides* bc_1 complex model (64) is constructed using the coordinates of subunit VII of the mitochondrial bc_1 complex's crystal structure.

However, according to the crystal structure of the bovine bc_1 complex, subunit VII is too far from the possible Q-binding sites to be a part of either the Q_o or the Q_i site. Although exact location of Q_o site is still controversial, it is generally believed to be in proximity to the binding positions of the Q_o site inhibitors, like myxothiazol or

stigmatellin. If the subunit IV of *R. sphaeroides* bc_1 complex is in the position as proposed in the model, the azido-Q binding fragment would be too far from the Q-binding sites. Therefore, it is still not clear how the Q-binding feature of subunit IV is involved in the functioning of the bc_1 complex.

To study the function of subunit IV, an *in vivo* gene complementation approach is used. We constructed a pRKD plasmid containing wild-type or mutated subunit IV gene (*fbc*Q), and introduced the complement into RSΔIV. The plasmid encoded subunit IV and the chromosome encoded cytochrome *b*, cytochrome c_1, and ISP would assemble *in vivo*. This *in vivo* reconstituted (or gene complemented) strain has the same features as the wild-type strain (61). Using site-directed mutagenesis on the subunit IV gene followed by *in vivo* reconstitution, we identified some essential amino acid residues involved in Q-binding or structural functions of subunit IV. Amino acid residues 6-11 are found to be essential for the structural function of subunit IV, Trp79 is found to be essential for the function of both structure and Q-binding, while Thr77, Tyr81, residues 2-5, and residues 113-124 are found to be not essential (65). However, when the deletion was extended more than 10 residues, the resulting mutant strain contained no subunit IV. Since the mRNA of the mutant subunit IV can be detected with Northern blots, the absence of subunit IV is likely due to the instability of the mutated subunits IV within the *R. sphaeroides* (65).

To solve the difficulty presented by mutagenesis studies by the *in vivo* reconstitution approach, an in vitro reconstitution approach was developed (66). The expression plasmid, pGEX/IV, is constructed by in frame ligation of subunit IV gene with the glutathione-S-transferase (GST) gene on the pGEX-2T plasmid. Under the control of the

tac promoter, the expression is inducible by isopropylthiogalactoside (IPTG). The expressed GST-subunit IV fusion protein can be purified from cell extract with glutathione-agarose gel. The purified recombinant subunit IV protein is then obtained by thrombin digestion of the fusion protein to remove GST. Reconstitution of the 3-subunits cytochrome bc_1 complex *in vitro* with this recombinant subunit IV has activity and property similar to those of wild-type complex. This is an indication that the recombinant subunit IV is functionally active and can be properly assembled into the active cytochrome bc_1 complex (66). By using site-directed mutagenesis coupled with *in vitro* reconstitution, it is possible to study the interaction of subunit IV and the 3-subunit core complex.

Electron Leakage and Superoxide Generation in the bc_1 Complex

It has been reported that about 1-2% of oxygen consumption during normal respiration is not involved with oxidative phosphorylation, but rather with the formation of superoxide (67). Complex I and Complex III (bc_1 complex) were identified as two segments responsible for much of the superoxide generated in mitochondria (68-71). In the bc_1 complex, ubisemiquinone radical (68) and reduced cytochrome b_{566} (or b_L) (69) are suggested as the autoxidizable factors causing superoxide production during the ubiquinol-cytochrome *c* reductase turnover.

Superoxide is a free radical capable of causing oxidative damage to the mitochondrion and cellular proteins, lipid, and nucleic acids. Also acute exposure to superoxide and other reactive oxygen species can inactivate the iron-sulfur clusters of

complex I, II, and III, resulting in shutdown of the mitochondrial respiratory chain (72). Superoxide and other reactive oxygen species generated in mitochondrion are reported to be related to diseases associated with respiratory chain or superoxide dismutases (SOD) abnormal functioning (72,73). However, under normal circumstances, the superoxide generated from mitochondria does little damage, since it is efficiently removed by SOD. In addition, generation of superoxide during respiration has two physiological purposes: regulation of membrane potential and maintenance of body temperature (35).

For bc_1 complex, the generation of superoxide could be under control if the ubisemiquinone or reduced cytochrome b_L are well protected from contact with oxygen. It is possible that the supernumerary subunits of bc_1 complex may provide such protection. Most studies of the superoxide generated by bc_1 complex are focused on its medical significance or on the enzymatic mechanism of the bc_1 complex. No one has reported the relationship between the superoxide generation by bc_1 complex and the supernumerary subunits of the complex. In this study, the involvement of subunit IV on reducing the electron leakage and superoxide generation is discussed.

The Purpose and Strategy of Study

The purpose of this study is to understand the role of the supernumerary subunit, subunit IV, in the cytochrome bc_1 complex from a photosynthetic bacterium *R. sphaeroides*. The specific aims are: 1) to identify amino acid residues of subunit IV involved in interaction with the 3-subunit core complex; 2) to investigate the effect of

subunit IV on the thermo-stability of the cytochrome bc_1 complex; 3) to investigate the role of the subunit IV in preventing electron leakage from the bc_1 complex.

Various subunit IV mutants were generated and characterized to identify the regions and individual amino acid residues of subunit IV required for interaction with the core complex to restore activity. The effect of the transmembrane helix region of subunit IV on its assembly into the complex was investigated by testing the association between subunit IV mutants and histidine-tagged 3-subunit bc_1 complex, which binds strongly to the Ni-NTA gel. The effect of ISP on the incorporation of subunit IV to the complex was also examined. The effect of subunit IV on the stability of the complex was investigated by differential scanning calorimetry (DSC). Mutations on certain critical amino acid residues of subunit IV were tested for their effect on activity restoration, incorporation with the core complex, and stability of the complex to understand their roles in subunit IV's function. To investigate the possibility that subunit IV is able to prevent electron leakage, the pre-steady state kinetic of quinol oxidation by bc_1 complex, and superoxide generation were studied by using stopped-flow kinetic analyzer coupled with the chemiluminescent reagent 2-methyl-6-(-*p*-methoxyphenyl)-3,7-ddihydroimidazo[1,2-α]pyrazin-3-one hydrochloride (MCLA) as a superoxide detecting agent.

CHAPTER II

MATERIALS AND METHODS

Growth of Bacteria

Rhodobacter sphaeroides

Plasmid bearing *Rs*ΔIV cells (61) were grown photosynthetically at 30°C in an enriched Sistrom medium containing 5 mM glutamate and 0.2% casamino acids. Cells were harvested with centrifugation at 3,500 x g for 30 minutes, when the turbidity (OD_{600nm}) of the cell culture reached 2.0. The harvested cells were then washed with 20 mM Tris-succinate buffer, pH 7.5, and stored at -20°C. About 5 – 6 grams of cells are routinely obtained from 1 liter of culture.

Antibiotics were added at the following concentrations: tetracycline, 10–15 mg/liter; kanamycin sulfate, 20 mg/liter; and trimethoprim, 25 mg/liter.

Escherichia coli

For general purpose, *E. coli* cells were grown aerobically at 37°C in LB medium. For the rescue of single-stranded DNA used in site-directed mutagenesis, *E. coli* cells were grown in TYP broth, which contained 16 g Bacto-trypton, 16 g Bacto-yeast extract, 5 g NaCl, and 2.5 g K_2HPO_4.

For over-expression of GST-subunit IV fusion protein, KS-1000 *E. coli* cells containing pGEX-2T/IV were grown with the following procedures. A 2.5 ml of overnight culture was inoculated into a 250 ml LB medium containing ampicillin in a 1000 ml flask. The culture was incubated at 37°C with shaking until the OD_{600nm} reached 0.6-0.8. The culture was then incubated in ice to stop the cell growth. Cells were collected with centrifugation and resuspended in 10 ml of fresh LB medium before being inoculated into a fermentor with 6 liters of LB medium containing 2% glucose. The fermentor was kept at 23°C with stirring and aeration. Several drops of antifoam solution (Sigma A5551) were added to avoid the formation of foam. When the OD_{600nm} of the culture reached 0.8 to 1.0 (usually 12-14 hours from inoculation), IPTG was added to final concentration of 0.2 mM. The cells were harvested by centrifugation at 3,500 x g for 30 minutes after 6 hours of IPTG induction, washed with 100 ml of PBS buffer, and stored at -20°C.

Antibiotics, when needed, were added at the following concentrations: ampicillin, 100–125 mg/liter; tetracycline, 10–15 mg/liter; kanamycin sulfate, 30–50 mg/liter; and trimethoprim, 85–100 mg/liter.

Construction of Expression Plasmid and Site-Directed Mutagenesis

Construction of *R. sphaeroides* Strains Expressing the His_6–Tagged 4-Subunit and 3-Subunit Cytochrome bc_1 Complexes

The expression plasmid for His-tagged four-subunit wild-type cytochrome bc_1 complex (pRKD*fbc*FBC_HQ) was constructed previously in our laboratory (30). A 1.2-kb

*Xba*I-*Hind*III fragment containing the *fbc*C and *fbc*Q genes from pRKD*fbc*FBCQ, containing *fbc*F, *fbc*B, *fbc*C, and *fbc*Q, was ligated into a modified pSELECT-1 vector in which the unique *Acc*65I (5'...G▼GTACC...3') site was eliminated. The resulting pSEL*fbc*CQ was used as template for site-directed mutagenesis to introduce an *Acc*65I recognition site right before the stop codon of the *fbc*C gene with Altered Sites *in Vitro* Mutagenesis System. Two complementary oligonucleotides with 6His tag coding sequence and the *Acc*65I overhang (5'...GTAC...3') attached at the 5'...ends (5'-GT ACG GGC CAT CAC CAC CAC CAT CAC TAA...3' and 3'...C CCG GTA GTG GTG GTG GTA GTG ATT CAT G...5') were synthesized, annealed together by heating up to 70 °C and cooling slowly to room temperature, and ligated into the *Acc*65I site of pSEL*fbc*CQ to generate pSEL*fbc*C_HQ. The 6-histidine insertion was confirmed by DNA sequencing. A 1.2-kb *Xba*I-*Hin*dIII fragment containing *fbc*C_HQ from pSEL*fbc*C_HQ was ligated into XbaI and HindIII sites to obtain pRKD*fbc*FBC_HQ.

The expression plasmid for the subunit IV-deficient, three-subunit core complex (pRKD*fbc*FBC_H) was generated by digestion of the pRKD*fbc*FBC_HQ plasmid with *Bam*HI and *Hind*III to remove the *fbc*Q gene, filling in with Klenow and annealing the ends.

The resulting pRKD*fbc*FBC_HQ and pRKD*fbc*FBC_H were transformed into *E. coli* S17, and then mobilized into *R. sphaeroides* BC17 and RsΔIV, respectively by parental conjugation to generate pRKD*fbc*FBC_HQ/BC17 and pRKD*fbc*FBC_H/RSΔIV. *R. sphaeroides* BC17 mutant has its entire *fbc* operon deleted from the chromosome (54); *R. sphaeroides* RsΔIV has its *fbc*Q gene deleted from the chromosome.

Construction of an *E. coli* strain Expressing the Subunit IV

Recombinant subunit IV is produced by *E. coli* Ks1000 cells carrying the pGEX/RsIV expression plasmid. Plasmid pGEX/RsIV was constructed previously in our laboratory by in-frame ligating subunit IV gene (*fbc*Q) with the GST gene in the pGEX2TH plasmid (66). In order to be able to in-frame ligate the fbcQ with the GST gene on the expression vector pGEX-2TH, a *Bam*HI recognition sequence (5'...G▼GATCC...3') was created by site-directed mutagenesis immediately up-stream from the start codon (ATG) of subunit IV on the plasmid pSelect/RSIV$_{BB}$, The resulting plasmid, pSelect/RSIV$_{BBB}$ was digested with *Bam*HI to produce a 505-base pair fragment containing *fbc*Q. This *Bam*HI fragment was ligated into pGEX-2TH to generate pGEX/RSIV. The plasmid was then transformed into *E. coli* KS1000, which is Prc protease deletion strain (74), to decrease the protease digestion of recombinant subunit IV. Colonies producing recombinant subunit IV were identified by immunological screening with antibodies against subunit IV.

Generation of *E. coli* Strains Producing Subunit IV Mutants with the Altered Site Mutagenesis System from Promega

Mutations on subunit IV gene were generated by using the single-strand pSelect/IV as a template, and a mutagenic oligonucleotide and an ampicillin repair oligonucleotide as DNA synthesis primers. The single-stranded template was prepared by infecting INVαF' *E. coli* cells containing plasmid pSelect/IV with R408 helper phage. The plasmid then enters the f1 replication mode and the resulting single-strand DNA was exported into the growth medium. The single-stranded DNA was then purified by PEG precipitation and phenol/chloroform extraction.

The mutagenic oligonucleotides, which were complementary to the single-strand template with the desired mutagenic mismatch located in the center, were synthesized (listed in Table I). Before annealing with the template, the mutagenic oligonucleotide was 5'-phosphorylated with T4 kinase to increase linkage between the mutagenic oligonucleotide and the ampicillin repair oligonucleotide, thereby increasing the chances of successful mutation.

The ampicillin repair oligonucleotide and the mutagenic oligonucleotide were annealed to the single-stranded template by heating the annealing mixture to 70° and then slowly cooling it down. Following the annealing, the mutant strand was synthesized and ligated by T4 DNA polymerase and T4 DNA ligase at 37°C for 90 minutes. The resulting heteroduplex DNA is then transformed into the repair minus *E. coli* strain BMH 71-18 *mut* S. Plasmid DNA was then isolated from the cells, which were grown overnight in the presence of ampicillin, and transformed into the JM109 strain. Mutants were confirmed by direct sequencing of the plasmid.

The resulting plasmid was digested with *Bam*HI to produce a 505-bp fragment containing mutated *fbc*Q gene. This *Bam*HI fragment was then ligated into the *Bam*HI site of pGEX-2TH. Orientation of the gene on the plasmid was confirmed by examining the product size of the *Eco*R I + *Sac* I digestion. The plasmid with the correct insert orientation would produce a 392 bp fragment instead of a 272 bp fragment.

Site-directed Mutagenesis on Subunit IV with Polymerase Chain Reaction (PCR)

PCR amplification was used to generate N-terminal truncated subunit IV mutants. Template and oligonucleotide primers used in the mutagenesis are listed in Table I. The forward primer contained the sequence prior to the *fbc*Q gene on the template and the

Table I. MUTATIONS OF SUBUNIT IV

Mutants	Mutagenesis methods[a]	Template	Primers
C-Terminal Truncation			
IV(1-40)	AS	pSelect/IV	CGCCTGGTGCAGAAATCGTGAGAGCTCCTCAAC[b]
IV(1-76)	AS	pSelect/IV	GCCAGCGCGATTTCGAGTGAGTCTGGAAATATC
IV(1-85)	AS	pSelect/IV	CGCTACCGCCTCTGAGGCTTCGCCTCG
IV(1-109)	AS	pSelect/IV	GGCAACTTCGGCGGCTGATCGGACGCCGGCAAC
N-Terminal Truncation			
IV(21-109)	PCR	pGEX/ IV(1-109)	f[c]:CCGCGTGGATCCGACCTCAGGAAA r:GAAAAGCTTCAGATGCGC
IV(41-109)	PCR	pGEX/ IV(1-109)	f:CCGCGTGGATCCCGCGAGCTCCTC r:GAAAAGCTTCAGATGCGC
IV(54-109)	PCR	pGEX/ IV(1-109)	f:CCGCGTGGATCCGCGACCTGGATC r:GAAAAGCTTCAGATGCGC
IV(77-109)	PCR	pGEX/ IV(1-109)	f:CCGCGTGGATCCACTGTCTGGAAATATCGCT r:GAAAAGCTTCAGATGCGC
IV(86-109)	PCR	pGEX/ IV(1-109)	f:CCGCGTGGATCCGGCGGCTTCGCC r:GAAAAGCTTCAGATGCGC
Alanine Scanning			
(41-47)A	QC	pGEX/IV	f:CGCCTGGTGCAGAAATCGGCCGCGGCCGCCGCCGCCGCGG AACTCAAGATCGATCC r:GGATCGATCTTGAGTTCCGCGGCGGCGGCCGCGGCCG ATTTCTGCACCAGGCG
(41-53)A	QC	pGEX/ IV(41-47)	f:GCCGCCGCCGCCGCGGCAGCCGCGGCCGCTGCTGCGACCT CCATCTGG r:CCAGATCCAGGTCGCAGCAGCGGCCGCGGCTGCCGCGGCG GCGGCGGC
(77-81)A	QC	pGEX/IV	f:GCCAGCGCGATTTCGAGGCTGCCGCGGCAGCTCGCTACCG CCTCCGGCG r:CGCCGAGGCGGTAGCGAGCTGCCGCGGCAGCCTCGAAATC GCGCTGGC
(77-85)A	QC	pGEX/ IV(77-81)	f:GAGGCTGCCGCGGCAGCTGCCGCCGCCGCCGGCGGCTTCC GCCTCGGGC r:GCCCGAGGCGAAGCCGCCGGCGGCGGCGGCAGCTGCCGCG GCAGCCTC
T77A	QC	pGEX/IV	f:CCAGCGCGATTTCGAGGCTGTCTGGAAATATCG r:CGATATTTCCAGACAGCCTCGAAATCGCGCTGG
V78A	QC	pGEX/IV	f:CGCGATTTCGAGACTGCCTGGAAATATCGCTAC r:GTAGCGATATTTCCAGGCAGTCTCGAAATCGCG

continued on next page

TABLE I continued

W79A	QC	pGEX/IV	f:GATTTCGAGACTGTCGCGAAATATCGCTACCGCCTC r:GAGGCGGTAGCGATATTTCGCGACAGTCTCGAAATC
K80A	AS	pSelect/IV	TTCGAGACTGTCTGGGCATATCGCTACCGCCT
Y81A	QC	pGEX/IV	f:GAGACTGTCTGGAAAGCTCGCTACCGCCTCGG r:CCGAGGCGGTAGCGAGCTTTCCAGACAGTCTC
R82A	QC	pGEX/IV	f:CTGTCTGGAAATATGCCTACCGCCTCGGCGG r:CCGCCGAGGCGGTAGGCATATTTCCAGACAG
Y83A	AS	pSelect/IV	GAAATATCGCGCCCGCCTCGG
R84A	AS	pSelect/IV	ATATCGCTACGCCCTCGGCGGCTT
L85A	QC	pGEX/IV	f:GAAATATCGCTACCGCGCCGGCGGCTTCGCCTCG r:CGAGGCGAAGCCGCCGGCGCGGTAGCGATATTTC
(82-85)A	QC	pGEX/IV	f:GAGACTGTCTGGAAATATGCCGCCGCCGCCGGCGGCTTCGC TCGGGC r:GCCCGAGGCGAAGCCGCCGGCGGCGGCGGCATATTTTCCAG CAGTCTC
(82-84)A	QC	pGEX/IV (82-85)A	f:GAAATATGCCGCCGCCCTCGGCGGCTTCGCCTCG r:CGAGGCGAAGCCGCCGAGGGCGGCGGCATATTTC
(81-84)A	QC	pGEX/IV (82-84)A	f:GAGACTGTCTGGAAAGCTGCCGCCGCCCTCGG r:CCGAGGGCGGCGGCAGCTTTCCAGACAGTCTC
Other Mutations			
W79F	QC	pGEX/IV	f:GATTTCGAGACTGTCTTCAAATATCGCTACCGCCTCG r:CGAGGCGGTAGCGATATTTGAAGACAGTCTCGAAATC
W79Y	QC	pGEX/IV	f:GATTTCGAGACTGTCTACAAATATCGCTACCGCCTCG r:CGAGGCGGTAGCGATATTTGTAGACAGTCTCGAAATC
Y81T	QC	pGEX/IV	f:GAGACTGTCTGGAAAACTCGCTACCGCCTCGG r:CCGAGGCGGTAGCGAGTTTTCCAGACAGTCTC
Y81F	QC	pGEX/IV	f:GAGACTGTCTGGAAATTTCGCTACCGCCTCGGC r:GCCGAGGCGGTAGCGAAATTTCCAGACAGTCTC
R82E	AS	pSelect/IV	GTCTGGAAATATGAGTACCGCCTCGGCGGCT
R82K	AS	pSelect/IV	GTCTGGAAATATAAGTACCGCCTCGGCGGCT
Y83T	QC	pGEX/IV	f:CTGGAAATATCGCACCCGCCTCGGCGGC r:GCCGCCGAGGCGGGTGCGATATTTCCAG
Y83F	QC	pGEX/IV	f:CTGGAAATATCGCTTCCGCCTCGGCGGC r:GCCGCCGAGGCGGAAGCGATATTTCCAG
R84E	QC	pGEX/IV	f:GTCTGGAAATATCGCTACGAGCTCGGCGGCTTCGCCTCG r:CGAGGCGAAGCCGCCGAGCTCGTAGCGATATTTCCAGAC
R84K	QC	pGEX/IV	f:GTCTGGAAATATCGCTACAAGCTCGGCGGCTTCGCCTCG r:CGAGGCGAAGCCGCCGAGCTTGTAGCGATATTTCCAGAC

a. AS, Alter Site Mutagenesis System; PCR, Polymerase Chain Reaction; QC, QuickChange Mutagenesis System

b. All primers are listed from 5' end to 3' end.

c. f, forward primer; r, reverse, primer.

sequence in the middle of the gene, therefore looped out part of the N-terminal sequence as desired. The reverse primer was complementary to the sequence following the *fbc*Q gene on the template. Consequently, the PCR product of this pair of primers with the *fbc*Q gene as template would be a double-strand DNA fragment containing *fbc*Q gene but without a certain part of its N-terminal sequence. To facilitate clone of the PCR product into the expression vector, the forward primer included a *Bam*H I site prior to the *fbc*Q gene, and the reverse primer included a *Hind* III site following the *fbc*Q sequence.

PCR amplification was performed in a MiniCycler^{TM} from M. J. Research. The thermal cycle was set-up as follows: step 1, 94 °C for 1 min; step 2, 92 °C for 40 sec for denaturation; step 3, 60 °C for 40 sec for annealing; and step 4, 75 °C for 90 sec for extension. A total of 30 cycles were performed with a final extension step of 5 min. The annealing time for the PCR amplification of the subunit IV(77–109) fragment was set for 70 s. PCR products were confirmed by size on agarose gel electrophoresis and cloned into the pCR cloning vector pCR2.1 from Invitrogen to generate pCR/IV$_m$ plasmids. The *Bam*H I-*Hind* III fragments from pCR/IV$_m$ plasmids were ligated into pGEX-2TH vectors to generate pGEX/IV$_m$ plasmids. These pGEX/IV$_m$ plasmids were individually transformed into *E. coli* KS1000. Mutations were confirmed by the size of the resulting GST-RSIV$_m$ fusion protein and the purified mutant subunit IV.

Site-Directed Mutagenesis on Subunit IV with QuickChange Mutagenesis System from Stratagene

For mutagenesis on subunit IV with the QuickChange system, the expression vector pGEX /IV was used as a template and two synthetic oligonucleotides containing the desired mutation were used as primers. All template and primers are listed in Table I.

The mutagenic oligonucleotide primers of exact complementation are supposed to anneal to the opposite strand of template and be extended during a thermal cycle with *Pfu* DNA polymerase. Therefore, a double strand mutant plasmid would be generated. Similar to regular PCR, the thermal cycle was set-up in a MiniCycler^{TM} from M. J. Research as follows: step 1, 98 °C for 30 sec for initiation; step 2, 98 °C for 30 sec for denaturation; step 3, decreasing temperature slowly (1 °C every 8sec) to 55 °C; step 4, 55 °C for 1 min for annealing; and step 5, 72 °C for 12 min for extension. Step 2 to 5 were repeated 18 times. Following the thermal cycle, the product was treated with restriction enzyme *Dpn* I. This digestion was used to select mutation-containing synthesized DNA, because DNA isolated from most of *E. coli* strains are *dam* methylated at adenine residues in the sequence 5'…G^{m}ATC…3' and therefore susceptible to *Dpn* I digestion, while the *in vitro* synthesized DNA is not. The *Dpn* I treated product was then transformed into XL1-Blue competent cells. Plasmid purified from a single XL1-Blue colony was sequenced to confirm the mutation and then transferred into *E. coli* KS1000.

Protein Purification

Purification of Histidine-Tagged 3-Subunit Core Complex and 4-Subunit Wild-Type Complex

Frozen *R. sphaeroides* cells harboring pRKD*fbc*FBC$_H$Q or pRKD*fbc*FBC$_H$ were suspended in 20 mM Tris-succinate, pH 7.5 (3 ml/g of cells), and passed twice through French press with at least 16,000 psi (1,000 psig with 1" diameter piston) to break open the cells. Protease inhibitor phenylmethylsulfinyl fluorid (PMSF), which routinely

prepared as 0.5 M in dimethyl sulfoxide (DMSO), was added to the cell suspension to a final concentration of 1 mM before passing through the French press, and was added to same concentration two more times after each passage through the French press. The broken cells were centrifuged at 40,000 xg (19,000 rpm with JA-20 rotor) for 20 minutes to remove unbroken cells and cell debris. The supernatant was then subjected to centrifugation at 220,000 x *g* (49,000 rpm with 50.2 Ti rotor) for 90 min to separate the chromatophore fraction from the soluble protein fraction. The ppt obtained was washed with 50 mM Tris-Cl, pH 7.5 containing 1 mM PMSF, and centrifuged at 220,000 x *g* for 90 min to recover the chromatophores in ppt. The resulting chromatophores were suspended in 50 mM Tris-Cl, pH 7.5 containing 1mM PMSF and 20% glycerol (final volume about 1ml for 1 g of cells), and stored at -80°C, until use.

To purify the His-tagged cytochrome bc_1 complex, the frozen chromatophore suspensions were thawed and adjusted to a cytochrome *b* concentration of 18 μM with 50 mM Tris-Cl, pH 7.5 containing 1 mM PMSF and 20% glycerol. Dodecylmaltoside (DM) solution (10%, w/v) was added to the chromatophore suspension to 0.66 mg/nmol of cytochrome *b*, and the mixture was stirred at 4 °C for 30 minutes. NaCl solution (4M) was added to a final concentration of 100 mM, and the suspension was stirred for another 30 minutes at 4°C. This mixture was centrifuged at 220,000 x *g* (49,000 rpm with 50.2 Ti rotor) for 90 minutes. The supernatant was collected and passed through a Ni-NTA agarose column (about 1 ml bed volume for every 100 nmol of cyt. *b* in the chromatophore suspension), equilibrated with 50 mM Tris-Cl, pH 7.5 containing 100 mM NaCl and 0.01% DM. The column, absorbed with bc_1 complexes, was then washed with 20 column volumes of the equilibrating buffer. The pure cytochrome bc_1 complex was

eluted with the equilibrating buffer containing 180 mM histidine, and concentrated to a final concentration of 300 μM cytochrome *b* or higher by using a Centriprep concentrator with a 30 kDa cut-off. For the experiment to test the association between 3-subunit bc_1 complex and subunit IV, the purified bc_1 complex was dialyzed against 50 mM Tris-Cl, pH 7.5 containing 100 mM NaCl and 0.01% DM to remove histidine. The purified complex was stored at -80°C in the presence of 20% glycerol.

Purification of Recombinant Subunit IV

Frozen KS-1000 *E. coli* cells (30-35 g for a typical batch) carrying the pGEX/RsIV plasmid were thawed and suspended in 100 ml of PBS (12 mM Na/K phosphate, pH 7.3 containing 140 mM NaCl and 2.7 mM KCl) and broken by passing through French press twice with at least 16,000 psi. PMSF (0.5 M in DMSO) was added to the cell suspension to a final concentration of 1mM, and added two more times after each French press passing. Triton X-100 was added to the broken cell suspension to a final concentration of 1%. The suspension was then incubated at 0 °C with stirring for 30 minutes and centrifuged at 40,000 x *g* (19,000 rpm with JA-20 rotor) for 20 min. The supernatant was collected and mixed with 30 ml of 50% glutathione-agarose gel slurry equilibrated with PBS. The mixture was gently shaken for 30 min at room temperature, and packed into a column (2.5 x 15 cm). After washing with 500 ml of PBS, the GST/subunit IV fusion protein was eluted from the column with 60 ml of 10 mM glutathione in 50 mM Tris-Cl, pH 8.0, and concentrated to a protein concentration of 10-15 mg/ml using Centriprep-10. The fusion protein was treated with thrombin (Sigma T-6884, 2 NIH unit/mg of fusion protein) at room temperature for 12 hours to release subunit IV from GST. After dialysis against PBS to remove glutathione from buffer, the thrombin-digested sample was first

treated with glutathione-agarose beads to partially remove the released GST and then subjected to a gel filtration with a Superdex-200 FPLC column equilibrated with 50mM Tris-Cl, pH7.5 containing 100 mM NaCl to completely remove GST and thrombin.

Determination of Protein Concentration

Lowry Method (75)

The protein sample was diluted to a concentration of 0.1-0.5 mg/ml. To 0.2 ml of the diluted protein sample, 1 ml of copper-alkali solution was added. The copper-alkali solution contained 0.01% of copper sulphate ($CuSO_4 \cdot 5H_2O$), 0.02% of sodium potassium tartrate, 0.1 M of sodium hydroxide and 2% of sodium carbonate. After mixing and incubating for 10 min, 0.05 ml of Folin-Ciocalteau's phenol reagent (Sigma F-9252) was added. The absorbance at 500 nm was read after 30 min incubation. BSA was used as a standard to estimate the protein concentration of the sample.

Bradford Method (76)

The protein sample was diluted to about 2-10 μg/ml. To 0.8 ml of a protein sample, 0.2 ml of Bio-Rad Protein Assay dye reagent (Bio-Rad #500-0006) was added. The reagent contained 0.01% Coomassie Brilliant Blue G-250 in 5% ethanol and 8.5 % phosphoric acid. After incubation for at least 5 min, the absorbance at 595 nm was read. BSA was used as the standard.

Absorbance at 280 nm

The protein concentration of purified wild-type subunit IV was estimated by measuring absorbance at 280 nm, using a millimolar extinction coefficient of 32.0 cm^{-1}.

This extinction coefficient was calculated according to the number of tryptophan (Trp) residues and of tyrosine (Tyr) residues in the wild-type subunit IV sequence (5 Trp and 3 Tyr) by the following equation:

$$\varepsilon_{280}\ [\mathrm{mM^{-1}cm^{-1}}] = 5.50 \times n_{\mathrm{Trp}} + 1.49 \times n_{\mathrm{Tyr}} \qquad (77)$$

For Subunit IV mutants whose composition of tryptophan and tyrosine has been altered, their extinction coefficients are calculated accordingly.

Determination of Cytochrome Content

The content of cytochrome *b* was determined from the sodium-dithionite-reduced-minus-potassium-ferric-cyanide spectrum using the extinction coefficient of 28.5 $\mathrm{cm^{-1}mM^{-1}}$ for wavelength pair 560 and 576 mm (78). The content of cytochrome c_1 was determined from the sodium-ascorbate-reduced-minus-potassium-ferric-cyanide spectrum using the extinction coefficient of 17.5 $\mathrm{cm^{-1}mM^{-1}}$ for wavelength pair 552 and 537 mm (79).

Enzymatic Activity Assay

The cytochrome bc_1 complex was diluted with 50 mM Tris-Cl, pH 7.5 containing 100 mM NaCl and 0.01% DM to a final concentration of cytochrome *b* of 3 μM. Appropriate amount (3-10 μl) of this diluted bc_1 complex was added to an assay mixture (1 ml) containing 100 mM sodium/potassium phosphate, pH 7.4 containing 0.3 mM EDTA, 100 μM cytochrome *c* (from horse heart, Sigma C-2506), and 25 μM $Q_0C_{10}BrH_2$. Ubiquinol-

cytochrome *c* reductase (QCR) activity of *R. sphaeroides* bc_1 complex was determined at room temperature (about 23°C) by measuring the reduction of cytochrome *c* by following the increase in absorbance at 550 nm and using a mM extinction coefficient of 18.5 cm^{-1}. Non-enzymatic reduction of cytochrome *c*, determined under the same conditions in the absence of enzyme, was subtracted. To measure bc_1 activity in chromatophores, 30 μM potassium cyanide was added to the assay mixture to inhibit the cytochrome *c* oxidase activity.

SDS-Polyacrylamide Gel Electrophoresis (PAGE)

SDS-PAGE for examining proteins smaller than 10 KDa was performed according to Schagger and von Jagow (80). Otherwise, SDS-PAGE was performed according to Laemmli (81).

Differential Scanning Calorimetry (DSC)

For DSC analysis, the bc_1 sample was diluted in phosphate buffer (Na/K Pi 100 mM, pH 7.4) instead of Tris buffer to avoid the large pH change during the heating. Prior to being loaded into the "sample cell" of a CSC Nano-DSC II, 0.6 ml of protein sample was degassed for 5 min to remove dissolved air, which may interfere with the DSC data during the heating process. The same volume of buffer was loaded into the "reference cell" of the instrument, after being degassed. During the scanning, both the sample and the buffer were heated from 10 °C to 90 °C, cooled back to 10 °C and heated again to 90

°C. The cells were equilibrated at 10 °C and 90 °C for 10 min before heating and cooling. The difference of power input between the "sample cell" and the "reference cell" was recorded in μW, with 1 data point taken every 10 seconds, as heating and cooling of the cells were done in a steady rate of 1°C per minute. The second heating scan was used as the baseline. Melting temperature (T_m) and enthalpy change (ΔH) of the sample were calculated by using the "CpCalc" program.

Pre-steady State Kinetics Measurements

Pre-steady state kinetics measurements were performed by stopped-flow spectroscopy using the Applied Photophysics SX.18MV stopped-flow spectrometer with a Photodiode Array accessory. Each reaction was started by mixing 50 μl of 6.0 μM bc_1 complex in 100 mM Na/K phosphate, pH 7.4 containing 0.01% DM, 0.1% BSA, 1mM KCN, and 1mM NaN_3 with an equal volume of 50 μM $Q_0C_{10}BrH_2$ in 5 mM NaH_2PO_4, 0.01% DM, 0.1% BSA, 1mM KCN, 1mM NaN_3, at 23°C. A spectrum from 600 nm to 500 nm, with a resolution of 2.17 nm was recorded every 1.25 msec. The dead time of the instrument was about 2 msec. The reduction of cytochrome *b* and c_1 was monitored with the absorption change in the wavelength pair 562-542 nm and 551-532 nm, respectively. The potassium ferric cyanide treated and sodium dithionite treated bc_1 complexes were used as references for 0 and 100% of reduction, respectively.

Superoxide Anion Radical Generation Measurement

To measure the superoxide radical generation during the electron transfer from quinol to the *b* or c_1 heme in the bc_1 complex, the complex and ubiquinol were mixed by the stopped-flow mixer in the same manner as described in the preceding section, except 0.4 μM MCLA was added to the quinol containing syringe. The generation of superoxide was monitored by detecting the chemiluminescence of the MCLA-superoxide adduct (82,83) with an emission photomultiplier on the stopped-flow spectrometer. The chemiluminescence was detected and recorded every 0.5 msec for 2 sec. Superoxide produced by the xanthine oxidase reaction with hypoxanthine as substrate was used as a standard for estimating the superoxide generation by the bc_1 complex.

CHAPTER III

LOCALIZTION OF REGIONS ESSENTIAL FOR INTERACTION WITH THE THREE-SUBUNIT CORE COMPLEX

Introduction

Purified 3-subunit core complex has a fraction of bc_1 activity of the 4-subunit wild-type complex. Addition of recombinant, wild-type subunit IV to the 3-subunit core complex restores the bc_1 activity to the same level as that of wild-type complex, indicates that the recombinant subunit IV is properly assembled into the complex. Thus, we can use the reconstitution active recombinant subunit IV to study its interaction in the bc_1 complex by site-directed mutagenesis coupled with *in vitro* reconstitution. In this chapter we report generation and characterization of subunit IV mutants which identify the regions of subunit IV required for interaction with the core complex to restore bc_1 activity. The topological arrangement of subunit IV in the chromatophore membrane is determined by monospecific polyclonal antibodies for various segments of subunit IV. The effect of the transmembrane helix region of subunit IV on its assembly into the bc_1 complex is investigated. The effect of Rieske iron-sulfur protein on the incorporation of subunit IV to the bc_1 complex is also examined.

Results and Discussion

Requirement of Residues 86-109 for Reconstitutive Activity of Subunit IV

To localize the regions required for reconstitutive activity, recombinant subunit IVs with progressive deletion of amino acid residues from the C-terminus were generated and characterized. These are: IV(1-109,), IV(1-85), IV(1-76), and IV(1-40), with deletions of 15, 39, 48, and 84 amino acid residues from the C-terminus of subunit IV, respectively.

These four C-terminal truncated subunit IV mutants are produced in *E. coli* as GST fusion proteins using constructed expression vectors, pGEX/IV(1-109), pGEX(IV(1-85), pGEX/IV(1-76), and pGEX/IV(1-40), respectively. These expression vectors were constructed by in-frame ligation of the subunit IV gene having the stop codon genetically engineered at positions 328-, 256-, 229-, and 121-bp down stream from the start codon, respectively, into the GST gene in the pGEX-2TH vector. The yield and purity of these four recombinant GST-mutant IV fusion proteins are comparable to that of GST-wild-type IV fusion protein (see Fig. 2A). Purified recombinant subunit IV mutants, IV(1-40), IV(1-76), IV(1-85), and IV(1-109) (see Fig. 2B) are obtained from their respective fusion proteins by thrombin cleavage and gel filtration.

Table II shows reconstitutive activities of the C-terminal truncated subunit IV mutants, with and without fused GST. Addition of purified recombinant IV(1-109) to the three-subunit complex restores the cytochrome bc_1 complex activity to the same level as that of the recombinant wild-type IV, suggesting that 15 amino acid residues (residues 110-124) on the C-terminus of subunit IV are not essential. This result is consistent with the *in vivo* gene complementation study which showed that deletion of residues 120-124

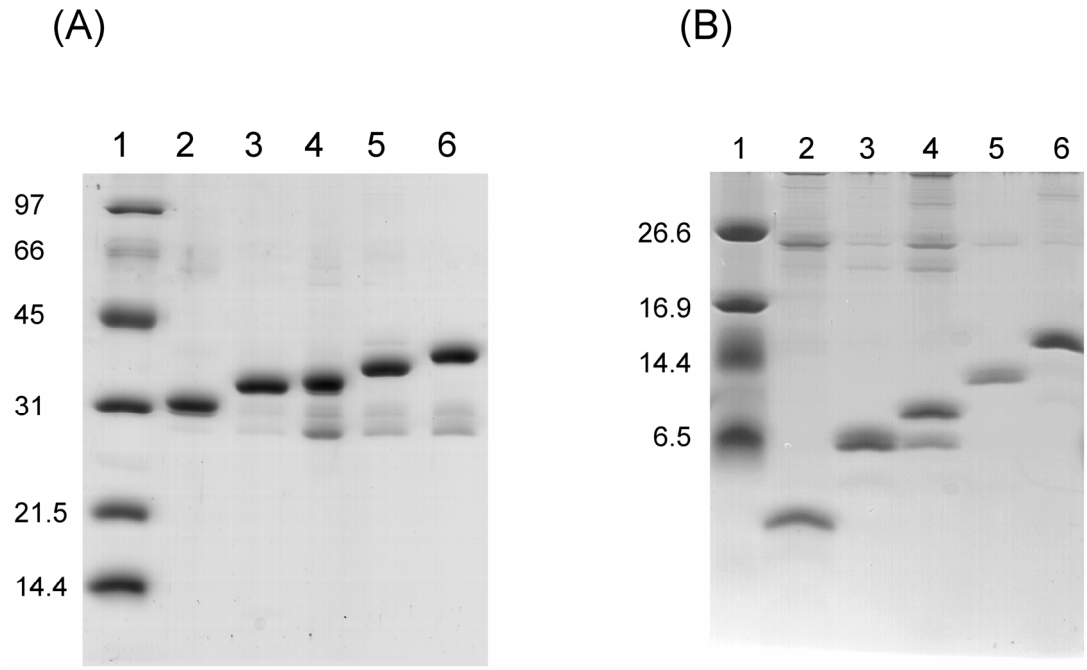

FIG 2. **SDS-PAGE of the C-terminal truncated subunit IVs, with and without fused GST.** A. Fused with GST on 12% Tris-Glycine gel: lane 1, protein standard: phosphorylase b (97,400), bovine serum albumin (66,200), ovalbumin (45,000), carbonic anhydrase (31,000), soybean trypsin inhibitor (21,500), and lysozyme (14,400); lane 2, GST-IV(1-40); lane3, GST-IV(1-76); lane 4, GST-IV(1-85); lane 5, GST-IV(1-109); lane 6, GST-wild-type IV(1-124). The SDS-PAGE system of Laemmli (81) was used. (B) Purified mutant proteins on 16% Tris-Tricine gel: lane 1, protein standard: triosephosphate isomerase (26,625), myoglobin (16,950), α-lactalbumin (14, 437), aprotinin (6,512), insulin b chain, oxidized (3,496), bacitracin (1,423); lane 2, IV(1-40); lane 3, IV(1-76); lane 4, IV (1-85); lane 5, IV (1-109); lane 6, wild-type IV (1-124).

Table II. Reconstitutive Activities of the C-Terminal Truncated Subunit IV Mutants.

Preparations	Reconstitutive Activity, %	
	Fused GST	Free
Wild type	100	100
IV(1-109)	99	97
IV(1-85)	8	0
IV(1-76)	6	0
IV(1-40)	0	0

The 100% reconstitutive activity is that restored by recombinant wild-type IV with or without fused GST.

Table III. Reconstitutive Activities of N-terminal truncated mutants of IV(1-109).

Preparations	Reconstitutive Activity, %	
	Fused GST	Free
Wild type	100	100
IV(1-109)	99	97
IV(21-109	95	90
IV(41-109)	98	96
IV(54-109)	53	n.d.
IV(77-109)	53	50
IV(86-109)	4	3
IV(86-124)	0	0

The 100% reconstitutive activity is that restored by recombinant wild-type IV or GST-wild type IV. n.d, not be determined due to protein aggregation.

of subunit IV does not impair the cytochrome bc_1 complex activity (61). While the IV(1-109) mutant possesses full reconstitutive activity, the IV(1-85) mutant shows no reconstitutive activity, indicating that residues 86-109 are essential. As expected, mutants IV(1-76) and IV(1-40) have no reconstitutive activity because the essential residues 86-109 are missing.

As shown in Table II, when these four C-terminal truncated subunit IVs fused with GST are added to the three-subunit core complex, the percent activity restoration is the same as when non-fusion proteins are added, indicating that the N-terminal portion of subunit IV may not be essential for its interaction with the three-subunit core complex.

Subunit IV Requires Its Transmembrane Helix Region for Assembly into the Cytochrome bc_1 Complex

Since residues 86-109 are essential for reconstitutive activity of subunit IV, it is important to elucidate the role this fragment plays during reconstitution. In the proposed structure of subunit IV (41), constructed based on hydropathy plots of the deduced amino acid sequence and possible α- and β- sheets, residues 86-109 comprise the only transmembrane helix. Therefore, the role of this fragment may be to provide membrane anchoring of subunit IV in the bc_1 complex. To confirm this speculation a His_6-tagged core complex was generated, characterized and used for incorporation studies of the C-terminal truncated subunit IVs, using Ni-NTA columns. The three-subunit core complex with a 6-histidine tagged at the C-terminus of cytochrome c_1 is constructed by deleting the subunit IV gene (*fbc*Q) from pRKD*fbc*FBC_HQ. The resulting plasmid PRKD*fbc*FBC_H is immobilized into an *R. sphaeroides* strain lacking the subunit IV gene (RSΔIV). The His_6-tagged core complex is purified from dodecylmaltoside solubilized chromatophores

in one step on a Ni-NTA column (66). The purity, activity, and cytochrome content of this His_6-tagged three-subunit core complex are similar to those of the un-tagged complex. However, the yield of purified His_6-tagged core complex is twice that from un-tagged bc_1 preparations and is obtained in 1/5 the time. When recombinant subunit IV is added to this His_6-tagged core complex, the extent of activity restoration is the same as that with the un-tagged complex, indicating that this His-tagged core complex is suitable for incorporation studies of recombinant subunit IV mutants.

When the His_6-tagged core complex is mixed with mutants IV(1-109), IV(1-85), IV(1-76), and IV(1-40), respectively, for 1 hr at 0 ^oC before being applied to Ni-NTA columns, the IV(1-109) is associated with the core complex in the same manner as the wild-type IV (see Fig. 3, lanes 2 &3), while IV(1-85) (see Fig. 3, lane 4), IV(1-76) and IV(1-40) (data not shown) do not associate with the His_6-tagged core complex. This result indicates that subunit IV requires its transmembrane helix region for assembly into the bc_1 complex. The lack of reconstitutive activity for mutants IV(1-85), IV(1-76) and IV(1-40) (see Table II) results from an inability of these mutants to bind to the complex because the transmembrane helix region is missing. The Rieske iron sulfur protein (ISP) was also reported to require its transmembrane helix for assembly into the bc_1 complex (84).

The Iron-Sulfur Protein Is Not Involved In the Association of Subunit IV with the bc_1 Complex

The finding that a purified two-subunit complex (cytochromes *b* and c_1), lacking both subunit IV and ISP, is obtained from chromatophores of mutants with altered ISP necks, either by deletion (ΔADV) (30,66) or double cysteine substitution (31), encouraged us to

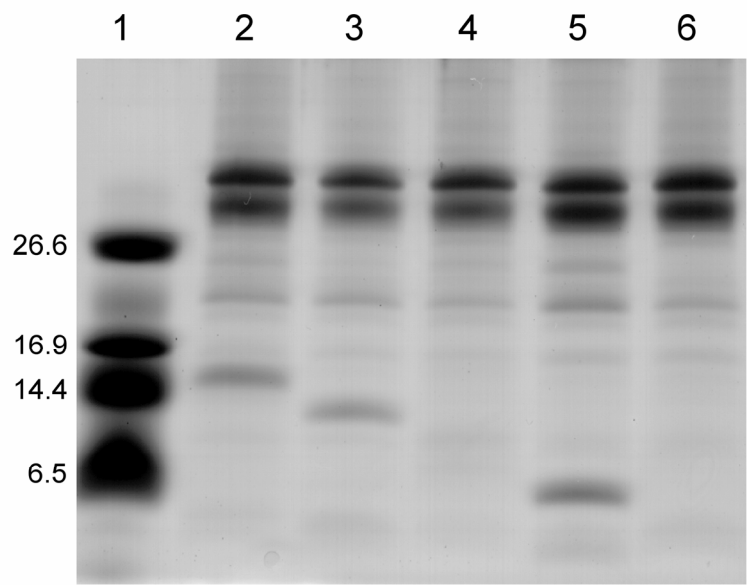

FIG 3. **SDS-PAGE of proteins eluted from Ni-NTA gels.** 3.0 µl aliquots of His_6-tagged three-subunit core complex, 30 mg/ml, containing 320 µM cytochrome *b,* were added 100 µl of buffer containing 42 µg of IV (1-124) (lane 2), 39 µg of IV(1-109) (lane 3), 33 µg of IV(1-85) (lane 4), 24 µg of IV(41-109) (lane 5), and none (lane 6). The mixtures were incubated at 4 ˚C for one hour and mixed with 0.2 ml of Ni-NTA gel. After washing the gel with 1 ml of B100 buffer (50 mM TrisCl pH 7.5, 0.01% dodecylmaltoside, 100 mM NaCl) twice, the proteins absorbed on the gel were eluted with 50 µl of B100 buffer containing 200 mM histidine, and subjected to SDS-PAGE. The protein standard is included in lane 1.

investigate the effect of ISP on incorporation of subunit IV. The His_6-tagged, three-subunit and two-subunit complexes were incubated with recombinant subunit IV at dodecylmaltoside concentrations ranging from 0.01% to 1%, for 1 hr at ˚C, and passed through Ni-NTA columns. The amount of subunit IV recovered in the column eluate of the three-subunit and the two-subunit complexes were the same (data not shown), indicating that incorporation of subunit IV into the bc_1 complex does need the presence of ISP. The simultaneous loss of ISP and subunit IV when the ISP neck is altered suggests that interaction between subunit IV and cytochrome *b* and/or c_1 involves ISP indirectly; alteration of the ISP neck may induce some changes on *b* or c_1 and thus decrease their affinity to subunit IV.

Identification of Residues 77-86 and 41-53 as Essential for Reconstitutive Activity of Subunit IV

Although the transmembrane helix region (residues 86-109) is required for subunit IV to be assembled into the bc_1 complex, addition of this fragment, generated by deletion of 85 amino acid residues from the N-terminus of IV(1-109) to yield IV(86-109), to the three-subunit core complex restores little bc_1 activity (see Table III). This suggests that the reconstitutive activity of subunit IV involves interaction with the core subunits after incorporation into the complex through the transmembrane helix. Since the IV(1-109) mutant has the same reconstitutive activity as that of recombinant wild-type IV, the interacting region must be in residues 1-85, as residues 86-109 are the transmembrane helix. Therefore, to identify the regions interacting with the core subunits, four other N-terminal truncated mutants of IV(1-109): IV(21-109), IV(41-109), IV(54-109), and IV(77-109), with progressive deletion of 20, 40, 53, and 76 amino acid residues were

generated and characterized. The purity and yield of IV(21-109), IV(41-109), and IV(77-109), isolated free (see Fig. 4B) or as the GST fusion proteins (see Fig. 4A), are comparable to those of recombinant wild-type IV or the IV(1-109) mutant. The IV(54-109), once cleaved from GST by thrombin digestion, becomes insoluble. Including 0.02% dodecylmaltoside in the fusion protein preparation during thrombin digestion did not prevent the released mutant protein from aggregation. The yield of recombinant IV(86-109) is low, about 10% of that obtained with recombinant wild-type IV, because a severe protease digestion occurred during the fusion protein preparation.

Table III compares maximum reconstitutive activities of mutants IV(86-109), IV(86-124), IV(77-109), IV(54-109), IV(41-109), and IV(21-109), with and without fused GST. Although the IV(86-109) mutant, which contains only the transmembrane helix, has little reconstitutive activity, the IV(77-109) mutant has 50% of the reconstitutive activity of the wild-type IV, indicating that residues 77-85 are involved in activation of the core complex. The increase in reconstitutive activity of the IV(77-109) mutant is not due to an increase in its hydrophilicity upon addition of residues 77-85 because the IV(86-124) mutant, with 15 down stream amino acid residues added to the transmembrane helix, has little or no reconstitutive activity. This result further confirms that residues 110-124 are not required.

The GST-IV(54-109) fusion protein has essentially the same reconstitutive activity as that of the GST-IV(77-109) fusion protein or IV(77-109) mutant, indicating that residues 54-76 are not essential. The IV(41-109) mutant has the same reconstitutive activity as the recombinant wild-type IV (a 2-fold increase of reconstitutive activity of the GST-IV(54-109) indicating that residues 41-53 are essential. As expected, the IV(21-109) mutant,

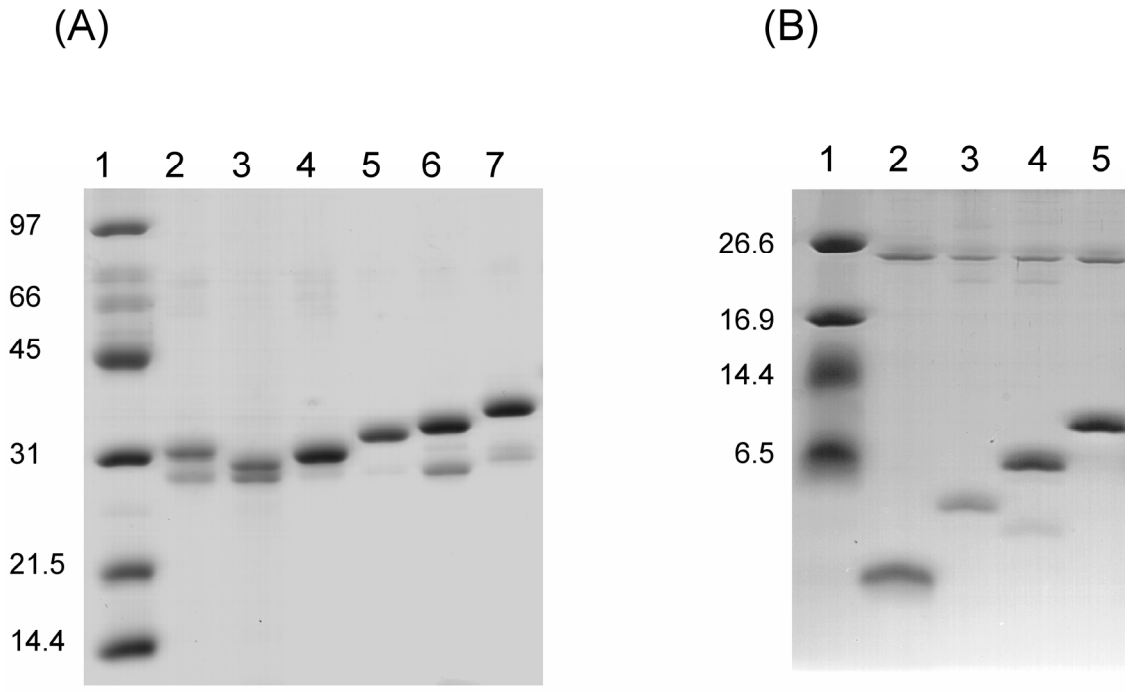

FIG.4.**SDS-PAGE of the N-terminal truncated mutants of IV(1–109) with and without fused GST.** *A,* fused with GST: *lane* 1, protein standard; *lane* 2, GST-IV(86–124); *lane* 3, GST-IV(86–109); *lane* 4, GST-IV(77–109); *lane* 5, GST-IV(54–109); *lane* 6, GST-IV(41–109); *lane* 7, GST-IV(21–109). *B,* purified mutant proteins: *lane* 1, protein standard; *lane* 2, IV(77–109); *lane* 3, IV(54–109); *lane* 4, IV(41–109); *lane* 5, IV(21–109). The SDS-PAGE systems and protein standards used were the same as described in the legend to Fig. 2.

with residues 21-40 added to the IV(41-109) mutant, has the same reconstitutive activity as that of wild-type IV, indicating that residues 21-40 are not involved in interacting with the core complex. Thus, two regions of subunit IV, residues 41-53 and 77-85, in addition to the transmembrane helix (residues 86-109), are essential for optimal interaction with the core complex to restore the bc_1 complex activity.

Localization of Interacting Regions of Subunit IV in the Proposed Structure of *R. sphaeroides* Cytochrome bc_1 Complex

Although the structural model for subunit IV (41) was constructed on hydropathy plots of its amino acid sequence, using the program of Kyte and Dolittle (85), and on predicted α and β helices, the sideness of the membrane is unknown. Lack of knowledge of the topological arrangement of subunit IV in the chromatophore membrane makes it difficult to localize the putative interacting regions of subunit IV in the bc_1 complex without the three-dimensional structure of this bacterial complex, which is not yet available. Therefore, the sideness of the membrane in the proposed structural model of subunit IV was determined using Fab'-horseradish peroxidase conjugates, prepared from antibodies against synthetic peptides corresponding to residues 59–73 (the near N-terminal peptide) and 110–124 (the C-terminal peptide), in sealed (inside-out) and broken chromatophores.

When sealed and broken chromatophore preparations are treated with Fab' fragment-horseradish peroxidase conjugates prepared from anti-C-terminal peptide antibodies, peroxidase activity is observed only with the broken chromatophores (Fig. 5), indicating that the C-terminal end is exposed on the periplasmic side of the chromatophore membrane. When sealed and broken chromatophore preparations are treated with Fab`

fragment-horseradish peroxidase conjugates prepared from anti-near N-terminal peptide antibodies, peroxidase activity is observed with both sealed and broken chromatophores (see Fig. 5), indicating that the N-terminal end is exposed on the cytoplasmic side of the chromatophore membrane. Thus, the first two putative interacting domains of subunit IV are on the cytoplasmic side of the chromatophore membrane (see Fig. 6). To further understand the subunit IV interaction with the core subunits, a three-dimensional structural model for the *R. sphaeroides* bc_1 complex (see Fig. 7) was constructed. The three core subunits are modeled using coordinates of beef heart mitochondrial cytochrome *b*, cytochrome c_1, and ISP, respectively, because of the sequence homology. Subunit IV is built in using the coordinates of subunit VII, which is functionally analogous. In this model, the three putative interaction domains of subunit IV are in close proximity to cytochrome b: the first domain is close to the DE loop, the second to helix G, and the third to helices H and G. Ionic interactions between Asp 46 (IV) or Asp 52 (IV), and Arg 231 (b) and between Glu 47 (IV) and Lys 234 (b) can be seen in the first interaction domain (Fig. 8, lower left). The interaction between the second domain of subunit IV and helix G of cytochrome b is through hydrogen bonding (Fig. 8, lower right). The backbone oxygens of Phe 428 and Ile 365 of cytochrome *b* form hydrogen bonds with Trp 79 , and Arg 84 of subunit IV, respectively. In addition, two oxygen atoms in the carboxylic acid group of Glu 425 of cytochrome b also form hydrogen bonds with Lys 80 of subunit IV. The interaction between the third domain and helices G and H of cytochrome b is hydrophobic (Fig. 8, upper right). Confirmation of these interactions will have to wait until the three-dimensional structure of this bacterial cytochrome bc_1 complex become available.

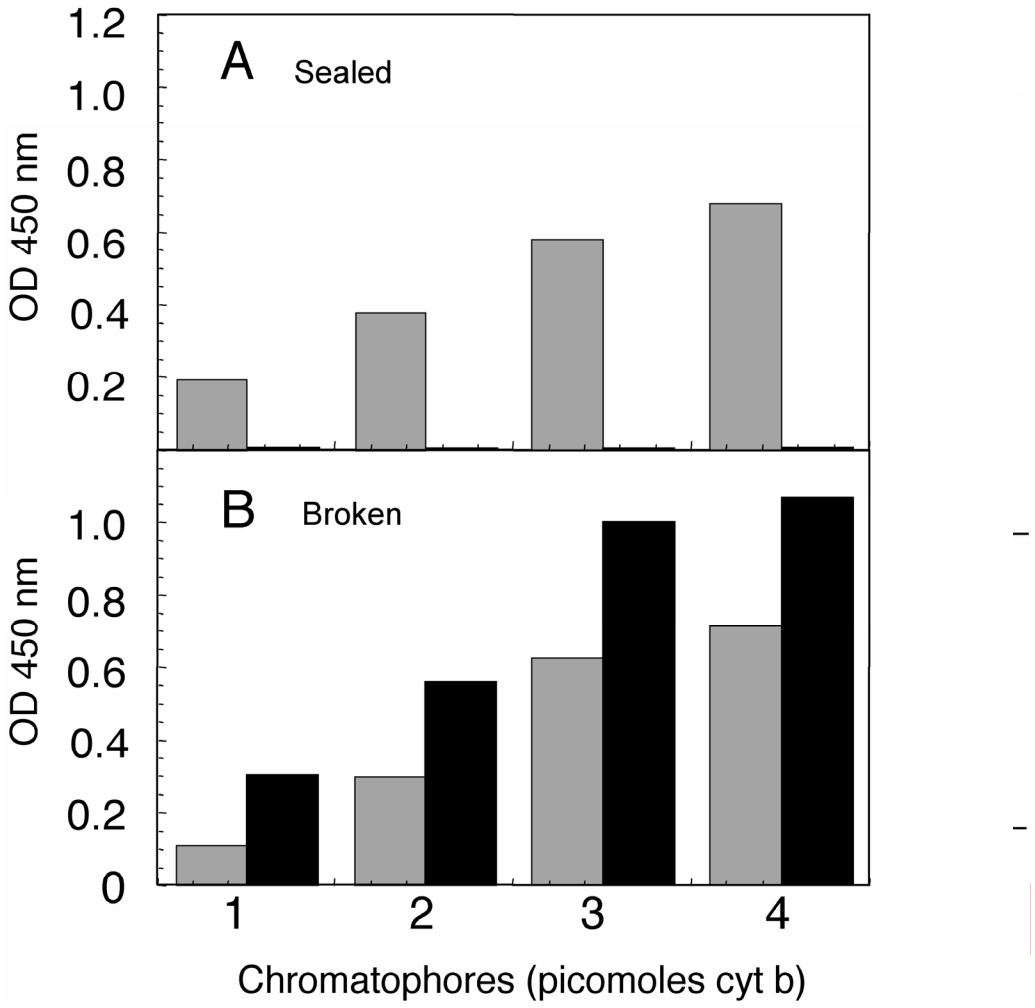

FIG.5. **Binding of Fab` fragment-horseradish peroxidase conjugates prepared from antibodies against a near N-terminal peptide (residues 59–73) *(gray bar*s) and the C-terminal peptide (residues 110–124) *(black bar*s) with sealed *(*A) and broken *(*B) chromatophores.** The indicated amounts of sealed and broken chromatophores were mixed with 10 mili units of Fab`-horseradish peroxidase conjugates prepared from anti-near N- or anti-C-terminal peptide antibodies in 50 mM sodium phosphate, pH 7.4, containing 0.25 M sucrose and incubated at 4 °C for 3 h. Mixtures were centrifuged at 30,000 x *g* for 15 min and the precipitate suspended in 50 mM sodium phosphate, pH 7.4, containing 0.25 M sucrose. This procedure was repeated for 3 more times before aliquots were assayed for horseradish peroxidase activity. Preimmune Fab`-horseradish peroxidase conjugate treated with sealed and broken chromatophores in an identical manner was used as control. The activities shown are after subtracting the control activity.

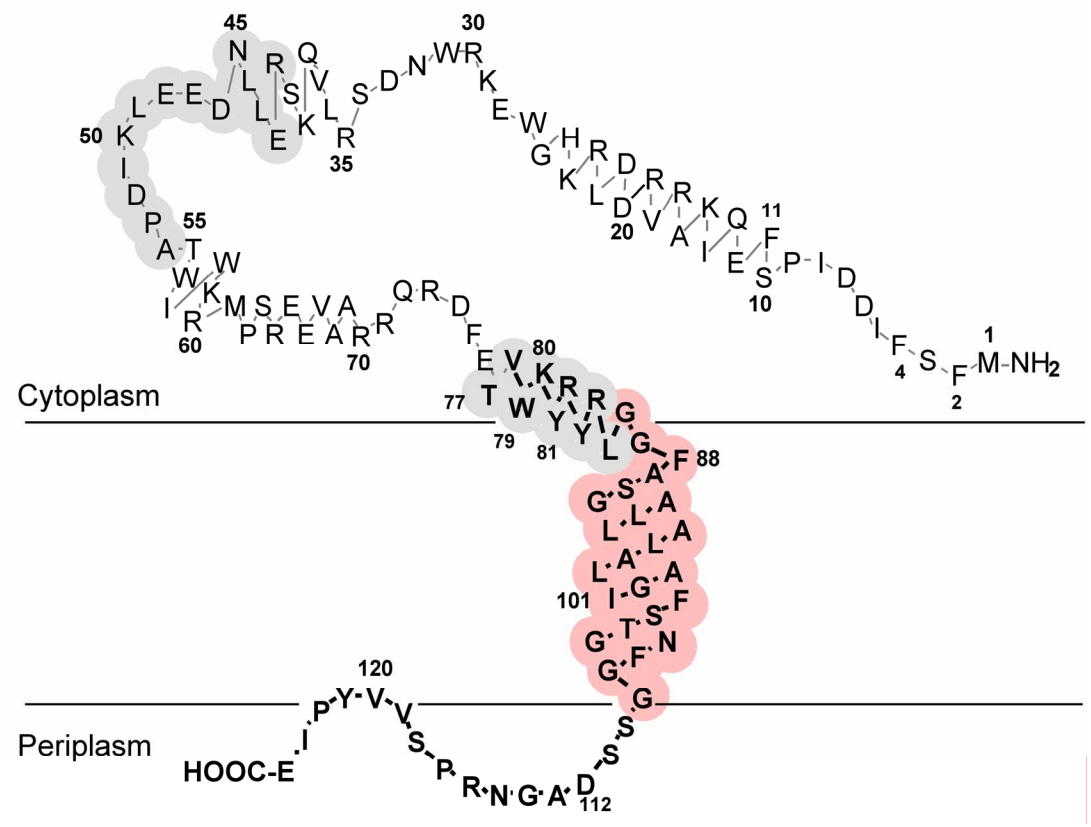

FIG. 6. **Localization of interacting regions of subunit IV in the proposed structural model of subunit IV in the chromatophore membrane.**

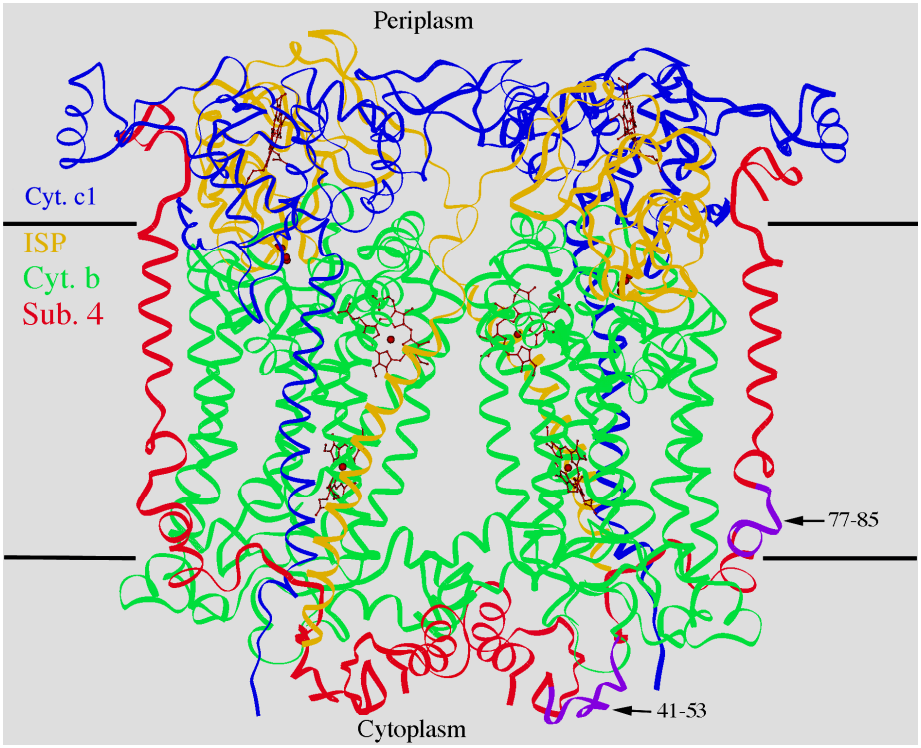

FIG.7. **Localization of interacting regions of subunit IV in the proposed three-dimensional structure of *R. sphaeroides* bc_1 complex.**

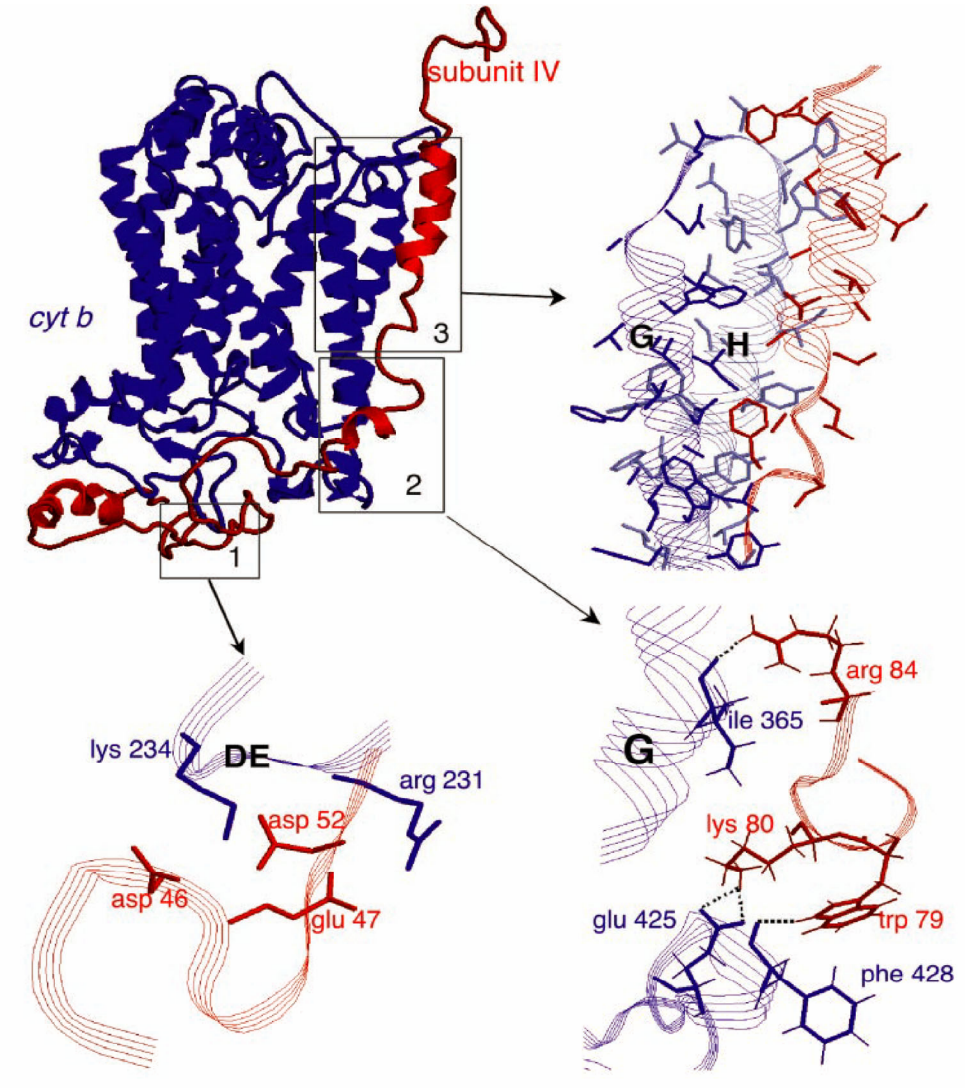

FIG.8. **The docking between sub-unit IV and cytochrome *b* in *R. sphaeroides* bc_1 complex.** Cytochrome *b* is indicated in *blue* and subunit IV is in *red*. The *boxed* areas (interaction regions) shown in the figure at the *upper left* are zoomed to make details visible.

CHAPTER IV

IDENTIFICATION OF AMINO ACID RESIDUES OF SUBUNIT IV INVOLVED IN INTERACTION WITH THE THREE-SUBUNIT CORE FROM *RHODOBACTER SPHAEROIDES*

Introduction

In the previous chapter, three regions of subunit IV; residues 41-53 (region I), 77-85 (region II), and 86-109 (region III) were found to be essential for the reconstitutive activity of subunit IV. Region III, which comprises the only transmembrane helix in the proposed model of subunit IV, is required for the incorporation of subunit IV into the bc_1 complex. However, addition of region III alone to the three-subunit core complex cannot restore the bc_1 activity, suggesting that reconstitutive activity of subunit IV requires interaction of regions I and II with the core complex after it is incorporated into the complex.

In continuing our efforts to understand the interaction between subunit IV and the core complex, we generated and characterized subunit IV mutants with alanine substitution at regions I and II. This was done to establish that the loss of reconstitutive activity in subunit IV mutants lacking region II, but not region I, is due to the essentiality

of the region, and not to improper protein assembly or folding resulting from the deletion. After the essentiality of region II is established, we used alanine scan in this region to identify amino acid residues involved in reconstitutive activity of subunit IV. We also generated and characterized subunit IV mutants to establish the functional groups of the identified essential residues in region II.

Results and Discussion

Tyrosine 81, Arginine 82, Tyrosine 83 and Arginine 84 Are Essential for the Reconstitutive Activity of Subunit IV

Previous studies indicate that three regions of subunit IV: residues 41-53 (region I), 77-85 (region II) and 86-109 (region III) are involved in interaction with the 3-subunit core complex to restore the bc_1 activity. Region III, which comprises the only transmembrane helix of subunit IV is shown to be required for subunit IV to incorporate into the complex, but the functions of Region I and II are not yet defined. However, a possibility exists that the loss of reconstitutive activity observed for the IV(54-109) and IV(86-109) might result from improper protein assembly or folding due to the large deletion rather than missing some specific amino acid residues on those two fragments. Therefore, to ensure that residues 41-53 and 77-85 of subunit IV are essential, recombinant subunit IV mutants with alanine substitution in these two regions were generated and tested for their ability to restore the bc_1 activity of the 3-subunit core complex. As shown in Table IV, when the IV(41-53)A mutant was mixed with the 3-subunit core complex, the bc_1 activity was restored to the same level as was done by the

wild-type subunit IV, indicating that residues 41-53 are not essential. The IV(77-85)A mutant restored only 15% of the activity restored by wild-type subunit IV. These results confirm that residues 76-85, but not residues 41-53, of subunit IV are essential for interaction with the core subunits of the bc_1 complex.

After confirming that residues 77-85 are required for reconstitutive activity of subunit IV, our next logic step would be to identify the essential amino acid residues in this region. To achieve this purpose, the recombinant subunit IV mutants with single alanine substitution at each residue from 77 to 85 were generated and determined for their reconstitutive activities. As shown in Table IV, when tyrosine 81, arginine 82, tyrosine 83 and arginine 84 are replaced individually with alanine, the subunit IV mutants have only about 80% of the reconstitutive activity of the wild-type subunit IV, while the subunit IV mutants T77A, W79A, and K80A have more than 95% of the reconstitutive activity, and V78A and L85A have more than 100% of the reconstitutive activity. These results indicate that Y81, R82, Y83, and R84 are essential for the reconstitutive activity of subunit IV. The subunit IV mutant (77-85)A, as mentioned above, has only 15% of the reconstitutive activity suggesting that the effect of the multiple mutations in this region are combination of the mutants with single alanine mutation. The subunit IV mutant (81-84)A, in which all the four essential residues were changed to alanine, lost 76% of the reconstitutive activity supporting the above suggestion.

Effect of the Mutations on the Interaction of Subunit IV with the Core Complex

To further investigate the interaction of the residues 77-85 of subunit IV with the core complex and ability to restore the bc_1 activity, the binding affinities of subunit IV mutants T77A, V78A, W79A, K80A, Y81A, R82A, Y83A, and R84A to the core complex,

Table IV. Reconstitutive activities of recombinant subunit IV mutants.

Subunit IV Mutants	Reconstitutive Activity*, %	Subunit IV Mutants	Reconstitutive Activity, %
Wild-type IV	100	Y81T	63
(41-53)A	106	Y81F	83
(77-85)A	15		
(81-84)A	24	R82E	56
T77A	95	R82K	95
V78A	105		
W79A	98	Y83T	58
K80A	97	Y83F	87
Y81A	83		
R82A	77	R84E	55
Y83A	80	R84K	100
R84A	76		
L85A	101		

*180 µl aliquots of histidine-tagged three subunit core complex, 3.3 µM cytochrome *b*, in TrisCl buffer, pH 7,5 containing 100 mM NaCl and 0.01% dodecylmaltoside, were mixed with 20 µl of purified recombinant wild-type and mutant subunit IV's, 60 µM, in 50 mM TrisCl buffer, pH 7.5, containing 100 mM NaCl, 0.01% dodecylmaltoside and 20% glycerol. The mixtures were incubated at 4°C for 1 h before the cytochrome bc_1 complex was assayed. The 100% reconstitutive activity represents the extent of activity increase as the 3-subunit complex reconstituted with wild-type subunit IV. Every result is average of at least three repetitions; the deviation between repetitions is typically less than 5%.

relative to that of wild type subunit IV, were determined. The availability of a His_6-tagged 3-subunit core complex in our laboratory enables us to use Ni-NTA for this study. The wild-type and mutant subunit IV's were mixed with the His_6-tagged core complex, at a molar ratio of subunit IV/cytochrome c_1 of 2. The reconstituted mixture contains 13.5 μM of the 3-subunit His_6-tagged complex and 27 μM of subunit IV. Two hundred μl aliquot of each of the reconstituted complexes was applied to three columns containing 150 μl of Ni-NTA gel equilibrated with 50 mM Tris-Cl, pH 7.5, containing 100 mM NaCl and 0.01% dodecylmaltoside. The columns were then washed with 20 column volumes of the buffer containing 0.01%, 0.02%, and 0.05% dodecylmaltoside respectively in 50 mM Tris-Cl buffer, pH 7.5, and 100 mM NaCl. The proteins absorbed to the columns were eluted with 50 mM TrisCl, pH 8.0, containing 180 mM histidine, 100 mM NaCl, and 0.01% dodecylmaltoside, and subjected to SDS-PAGE. The amount of subunit IV remaining in the column effluent was quantified by its intensity on gel with Coomassie blue staining.

Fig. 9-A, B, and C show SDS-PAGE patterns of proteins eluted from Ni-NTA columns after washing with buffer containing 0.01%, 0.02% and 0.05% dodecylmaltoside respectively. The amounts of subunit IV (both wild-type and mutants) recovered in the Ni-NTA column effluents decrease as the concentrations of dodecylmaltoside used in the washing step was increased. On the other hand, little change in the amounts of the core subunits (cyt. *b*, cyt. c_1, and ISP) was observed. In Fig.9-A, after the 0.01% DM wash, all subunit IV mutants recovered in the column effluent were comparable to the wild-type subunit IV, except for IV(Y83A) and IV(R84A), which were apparently less. As the DM

FIG. 9. **SDS-PAGE of reconstituted bc_1 eluted from Ni-NTA columns after washing with various concentration of dodecylmaltoside.** One hundred fifty-µl aliquots of His_6-tagged three-subunit core complex, 18 µM cytochrome c_1, were added to 50-µl of TNDG buffer (50 mM Tris-Cl, pH 7.5, containing 100 mM NaCl, 0.01% dodecylmaltoside, and 20% glycerol) containing no subunit IV (lane N), 5.4 nmol of wild-type subunit IV (lane W), mutant subunit IV T77A (lane 77), V78A (lane 78), W79A (lane 79), K80A (lane 80), Y81A (lane 81), R82A (lane 82), Y83A (lane 83), R84A (lane 84) or L85A (lane 85). After 1 hour incubation at 4 °C, the mixture of each reconstituting sample was applied to columns containing 150 µl of Ni-NTA gel equilibrated with TND (50 mM TrisCl buffer, pH 7.5, containing 100 mM NaCl and 0.01% dodecylmaltoside). Columns were washed with 3 ml of 50 mM TrisCl buffer, pH 7.5, containing 100 mM NaCl and (A) 0.01%, (B) 0.02%, or (C) 0.05% dodecylmaltoside, respectively. After washing, the proteins absorbed on the columns were eluted with 150 µl of TND containing 180 mM histidine and subjected to SDS-PAGE. The protein standard: bovine serum albumin (66,200), ovalbumin (45,000), carbonic anhydrase (31,000), soybean trypsin inhbitor (21,500) and lysozyme (14,400), is in line S.

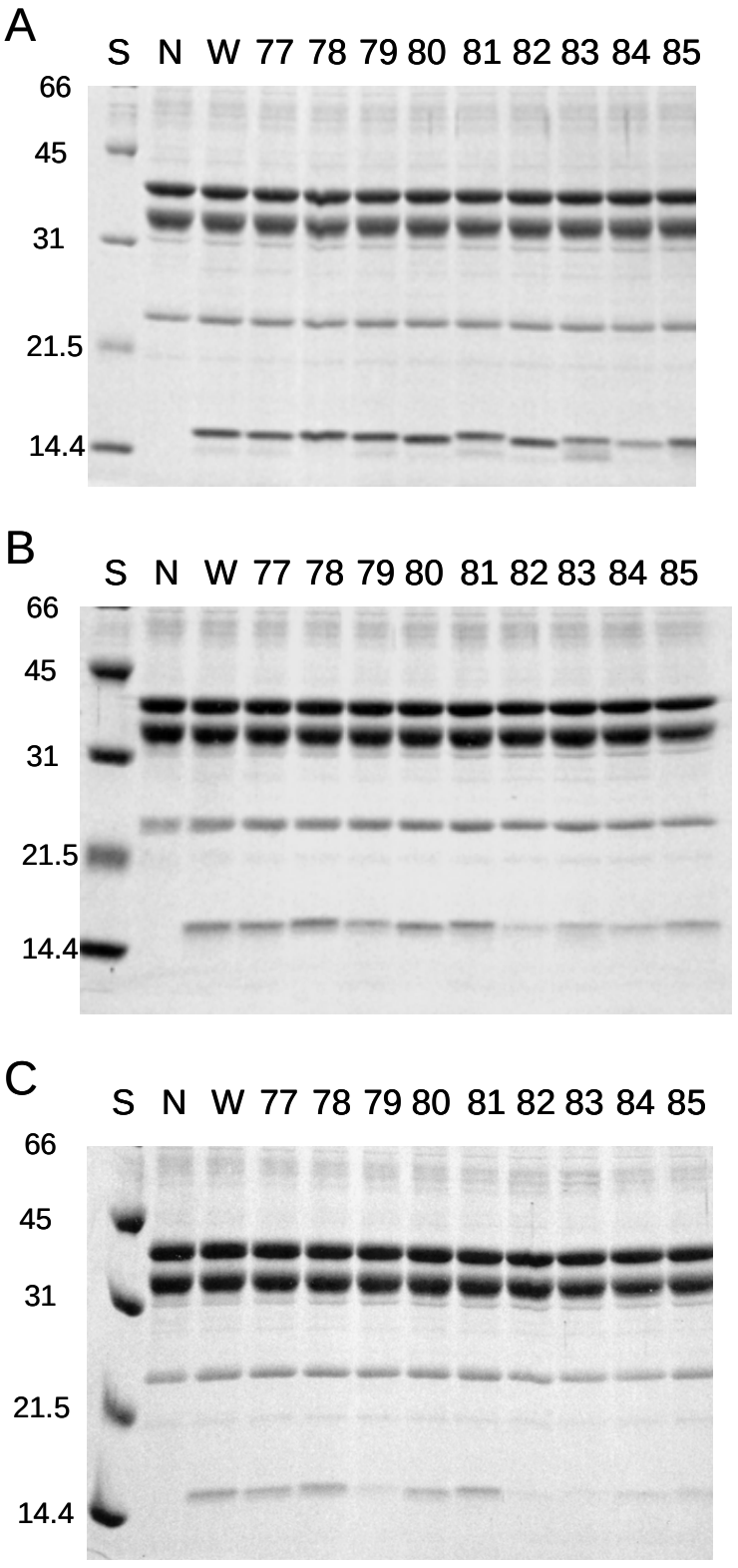
A
S N W 77 78 79 80 81 82 83 84 85
66
45
31
21.5
14.4
B
S N W 77 78 79 80 81 82 83 84 85
66
45
31
21.5
14.4
C
S N W 77 78 79 80 81 82 83 84 85
66
45
31
21.5
14.4

concentration in the washing buffer is increased to 0.02% and 0.05%, the amount of subunit IV mutants IV(W79A), IV(R82A), and IV(L85A) recovered in the column effluents decrease significantly upon comparison with wild-type subunit IV (Fig. 9-B and C). Therefore, subunit IV mutants IV(W79A), IV(R82A), IV(Y83A), IV(R84A), and IV(L85A) apparently show weaker binding to the core complex, as compared to wild-type subunit IV. Among these weakly bound subunit IV mutants, IV(R82A), IV(Y83A) and IV(R84A) were also found to have lower reconstitutive activity as mentioned in the previous section. Therefore, it is likely that the decrease in the reconstitutive activity of the IV(R82A), IV(Y83A), and IV(R84A) results from the decrease in binding affinity of these subunit IV mutants.

However, with up to 0.05% DM wash, the amount of the mutant IV(Y81A) remains the same as that of the wild-type subunit IV, as shown in Fig. 9. Therefore, the decrease in reconstitutive activity observed for the IV(Y81A) mutant seems to be unrelated to the decrease of the binding affinity of this mutant IV to the core complex. The reason for low reconstitutive activity of the mutant IV(Y81A) is still not clear.

In addition, the amount of IV(W79A) and IV(L85A) associated with the core complex also decreased after the reconstituted mixture in the Ni-NTA column was washed with 0.05% DM. However, in the reconstitutive activity test (Table IV), these two mutants showed no significant activity loss. Apparently, the tryptophan 79 and leucine 85 are required for the binding of subunit IV to the core complex, but the conditions in the reconstitutive activity test were not stringent enough to show reconstitutive activity loss of the subunit IV mutants W79A and L85.

Effect of the Subunit IV on the Thermostability of Cytochrome bc_1 Complex

Fig. 10 shows DSC thermograms of the 3-subunit core complex, reconstituted 4-subunit complex. The DSC thermogram of wild-type 4-subunit complex (not shown here) is comparable to that of the reconstituted complex. All of them show symmetrical endothermal transition peaks. The 4-subunit complex denatures at 46.4 °C, which was significantly higher than the melting temperature (T_m) of the 3-subunit complex at 42.1 °C. With a T_m higher by 4.3 °C, the complex with subunit IV is more stable than the complex without subunit IV. In addition to the melting temperature, the values of the total enthalpy change (ΔH), which represent the energy needed to complete the denaturation and are calculated from the area under the endothermal peak, are significantly different. While the reconstituted 4-subunit bc_1 complex has ΔH of 97 kcal/mol, the ΔH of the 3-subunit bc_1 complex is only 55 kcal/ mol. The energy difference between these two ΔH's suggests that there could be several bonds created either inside the core complex, or between the core complex and subunit IV, as the subunit IV is incorporated into the position. Therefore, the DSC analysis of a reconstituted bc_1 complex is a good indicator for how well a mutant subunit IV assembled itself into the complex.

DSC Studies of bc_1 Complexes Reconstituted with Subunit IV Mutants

All the subunit IV mutants were reconstituted with the 3-subunit core complex and subjected to DSC analysis under the same condition mentioned in the previous section. The thermal parameter results of these analyses are shown in Table V. DSC data of the complex with IV(41-53)A was comparable to that of the complex with wild-type subunit IV. This observation further confirms that the alteration of all the amino acid side-chains

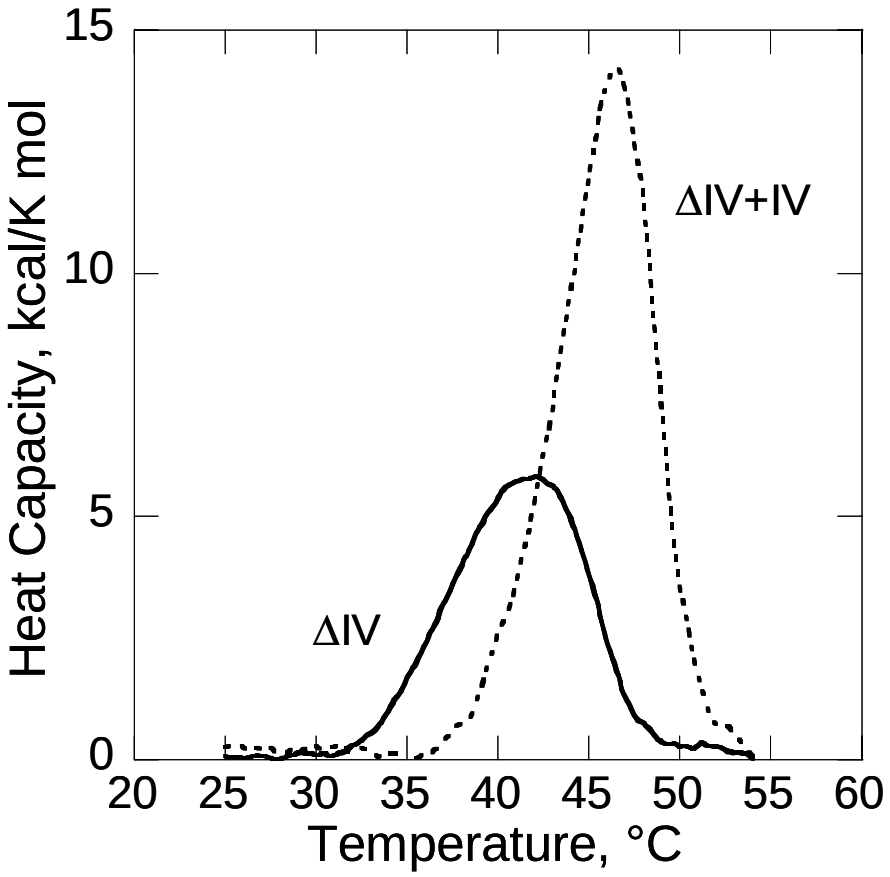

FIG. 10. **DSC thermograms of reconstituted bc_1 complexes.** The solid line is the DSC thermogram of histidine tagged 3-subunit cytochrome bc_1 complex with concentration of cytochrome *b* equaling to 30 μM in 83 mM phosphate, 8 mM TrisCl pH 7.4/ 17 mM NaCl/ 0.002% DM/ 3.3% glycerol. The dashed line is the DSC thermogram of the same sample in the same condition but with 40 μM of recombinant subunit IV in the sample.

Table V. DSC thermal parameters of bc_1 complexes with wild-typed or mutant subunit IV

Protein	T_m, °C	ΔH, kcal/mol	Protein	T_m, °C	ΔH, kcal/mol
ΔIV	42.1	55	ΔIV+IV(W79Y)	46.2	99
wt	46.4	99	ΔIV+IV(W79F)	45.5	89
ΔIV+IV wt	46.4	97			
ΔIV+IV(41-53)	46.3	96	ΔIV+IV(Y81T)	43.8	84
ΔIV+IV(77-85)	43.0	61	ΔIV+IV(Y81F)	45.4	95
ΔIV+IV(81-84)	42.3	68			
ΔIV+IV(T77A)	46.5	99	ΔIV+IV(R82E)	43.9	84
ΔIV+IV(V78A)	45.5	90	ΔIV+IV(R82K)	45.3	91
ΔIV+IV(W79A)	44.4	82			
ΔIV+IV(K80A)	45.3	95	ΔIV+IV(Y83T)	43.8	88
ΔIV+IV(Y81A)	44.8	93	ΔIV+IV(Y83F)	45.3	96
ΔIV+IV(R82A)	45.7	87			
ΔIV+IV(Y83A)	44.3	93	ΔIV+IV(R84E)	43.2	68
ΔIV+IV(R84A)	43.3	74	ΔIV+IV(R84K)	46.2	98
ΔIV+IV(L85A)	45.2	99			

on the region 41-53 of subunit IV to simple methyl groups has little effect on the interaction between subunit IV and the core complex. As expected, the complex with either IV(77-85)A, or IV(81-84)A have significantly lower T_m and ΔH value, when those critical residues were changed to alanine.

All single alanine mutants, except IV(T77A), more or less affect DSC parameters. Complex reconstituted with mutant IV(R84A) has a T_m of 43.3 °C, which is the lowest among all the single alanine mutants. This result is consistent with the incorporation test (see Fig 9), and it indicates that the mutation R84A has the most impact on the incorporation. The mutant IV(Y81A) shows no significant difference from the wild-type subunit IV in the incorporation test (see Fig. 9), but it lowers the complex's T_m by 1.6 °C upon comparison with wild-type subunit IV. The difference in T_m suggests that the alanine mutation at Y81 does affect the interaction between subunit IV and core complex, although the IV(Y81A) is still able to strongly bind to the core complex as the wild-type IV.

Significance of Ionic Property of R82 and R84

When the positively charged side-chain on R82 or R84 is replaced with the neutral methyl side-chain, the subunit IV mutant loses about 20% of the reconstitutive activity (Table IV), and has a weaker association with the core complex than wild-type subunit IV (Fig. 9). Therefore, it is reasonable to consider that the positive charge in this proximity may be important for the reconstitution of the subunit IV with the core complex.

To investigate the effect of the positively charged side-chain of arginine 82 and 84, subunit IV mutants IV(R82E), IV(R82K), IV(R84E), and IV(R84K) were constructed and characterized. As shown in Table IV, when arginine 82 is changed to the negatively

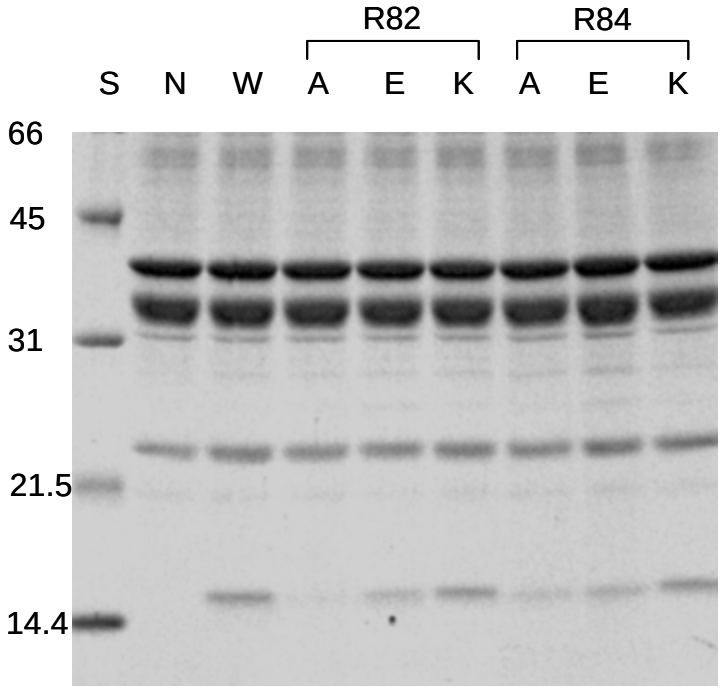

FIG. 11. **Effect of mutation at R82 and R84 on the association of subunit IV with the complex.** Conditions were as same as described on Fig. 9. Cytochrome bc_1 was reconstituted with none (lane N), wild-type (lane W), mutant IV at R82 (R82A, E, K) or mutant IV at R84 (R84A, E, K). Ni-NTA columns were washed with buffer containing 0.05% dodecylmaltoside before the elution. S, protein standard: bovine serum albumin (66,200), ovalbumin (45,000), carbonic anhydrase (31,000), soybean trypsin inhbitor (21,500) and lysozyme (14,400).

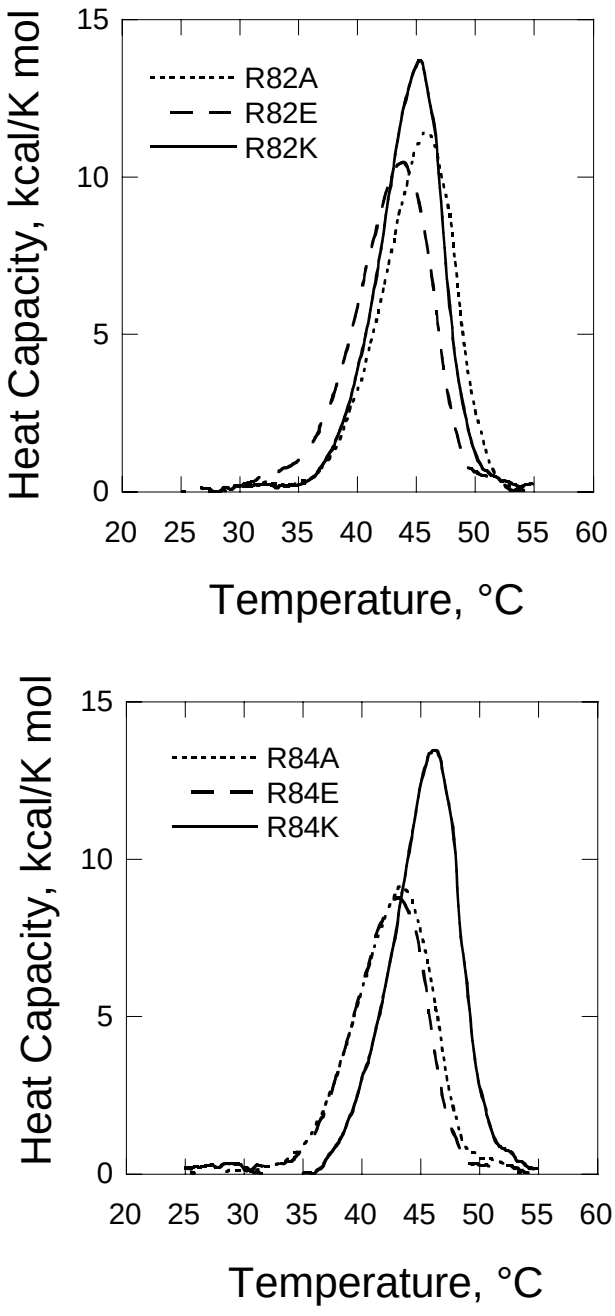

FIG12. **DSC thermograms of bc_1 complexes with mutants at R82 and R84.** Experiment conditions were as same as on Fig. 10.

charged glutamic acid, the reconstitutive activity drops to 56% of the reconstitutive activity of the wild-type subunit IV. When arginine 82 is changed to another positively charged residue, lysine, the reconstitutive activity increases to 95%. Similar effects are also observed when mutating arginine 84; the glutamic acid mutant drops the reconstitutive activity to 55%, and the lysine mutant increases the reconstitutive activity to 100%. These results reveal the significance of the positive charge on both arginine 82 and arginine 84.

To determine their binding affinity to the core complex, the subunit IV mutants R82A, R82E, R82K, R84A, R84E, and R84K were reconstituted with the His-tagged 3-subunit complex and applied to Ni-NTA columns as described above. Fig. 11 shows SDS-PAGE patterns of reconstituted proteins eluted from Ni-NTA columns after washing with buffer containing 0.05% DM. The amounts of both IV(R82K) and IV(R84K) shown on the gel are comparable to that of the wild-type subunit IV. This confirms the significance of the positively charged group of these two residues for the interaction between subunit IV and the core complex. However, IV(R82E) and IV(R84E), surprisingly show slightly stronger binding to the core complex than IV(R82A) and IV(R84A) do, as shown in Fig. 11. Since the mutation of arginine 82 or 84 to glutamic acid has a more drastic effect on the reconstitutive activity of the subunit IV than the mutation to alanine, it remains unclear why they would have a better association with the 3-subunit core complex.

Fig. 12 shows the DSC thermograms of the bc_1 complex reconstituted with the subunit IV mutants at R82 and R84. When R82 or R84 of the subunit IV is mutated to lysine, the thermogram of the reconstituted complex is comparable to the complex

reconstituted with the wild-type subunit IV. However, the thermogram of the complex with either IV(R82A), IV(R82E), IV(R84A), or IV(R84E) show significant differences from the complex with the wild-type subunit IV. Conclusively, the positive charge of arginine at both 82 and 84 are significant for the function of the subunit IV in interacting with the core complex.

Function of W79, Y81, and Y83

Although the mutant IV(W79A) has the same reconstitutive activity as the wild-type subunit IV, this mutation significantly decreases the binding affinity of the subunit IV to the core complex (see Fig. 9-C) and lowers the T_m of the complex as seen in DSC analysis (see Table V). To study the function of this tryptophan, two mutants, IV(W79Y) and IV(W79F) were constructed and characterized. As shown in Table V and Fig. 13, a tyrosine at position 79 is comparable to the tryptophan, and a phenylalanine is better than an alanine but not as good as a tryptophan or tyrosine. Apparently, the aromatic side chain is essential for the function of W79.

For the residues tyrosine 81, neither threonine nor phenylalanine is comparable to the tyrosine (see Table IV and Table V), suggesting that both the aromatic ring and the hydroxyl group of Y81 are required for its proper function.

Similar results were observed when the tyrosine 83 was replaced with threonine or phenylalanine, indicating the significance of both the aromatic ring and the hydroxyl group of the Y83. However, the mutant IV(Y83F) has 87% of reconstitutive activity, which is slightly higher than 80% of the IV(Y83A) and significantly higher than 66% of the IV(Y83T) (see Table IV). In addition, the association test (Fig. 14-A) shows that the IV(Y83F) binds the 3-subunit complex stronger than the IV(Y83A) and the IV(Y83T);

the DSC analysis (Fig.14-B) also shows that the complex with the IV(Y83F) has higher melting temperature than the complexes with the other two subunit IV mutants. Conclusively, although neither phenylalanine nor threonine can replace the function of the tyrosine at position 83 of the subunit IV, the aromatic ring of the tyrosine 83 apparently is more important than the hydroxyl group.

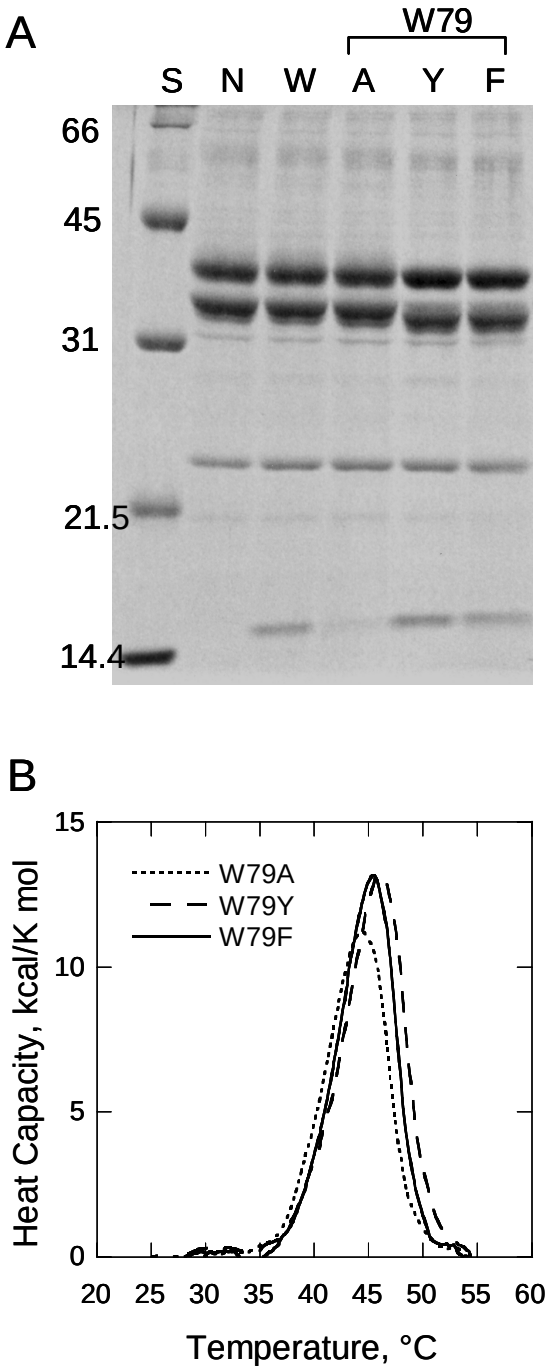

FIG. 13. **Effect of mutation at the W79 on (A) the association of subunit IV with the complex and (B) DSC thermograms.** Conditions are as same as described on Fig. 11 and Fig. 10.

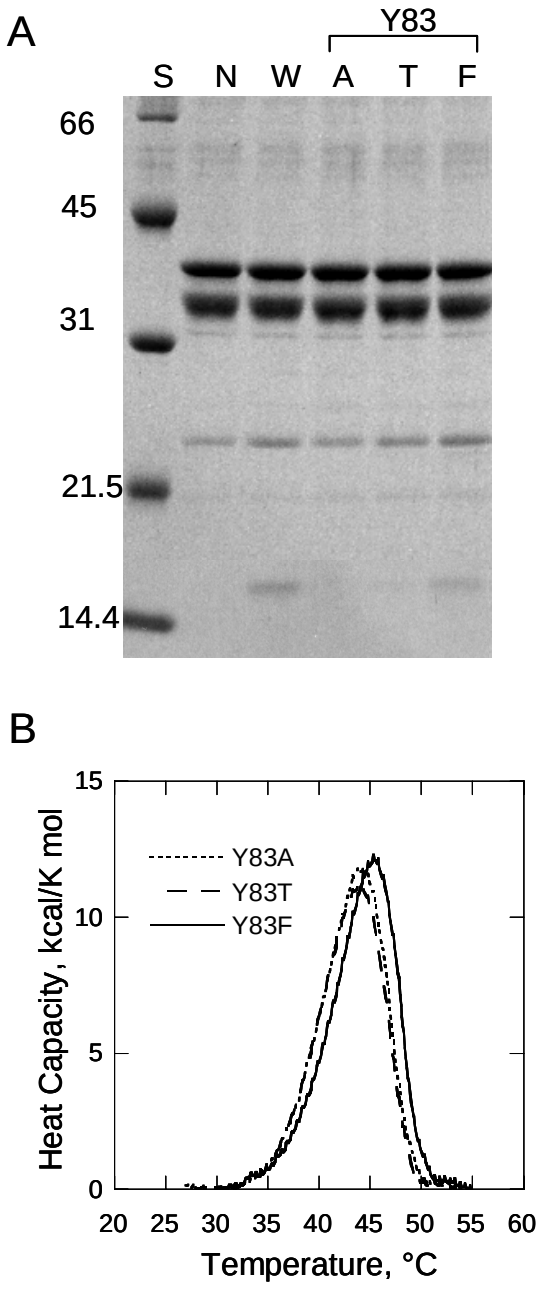

FIG. 14. **Effect of mutation at the Y83 on (A) the association of subunit IV with the complex and (B) DSC thermograms.** Experiment conditions are as same as on Fig. 11 and Fig 10.

CHAPTER V

SUBUNIT IV REDUCES THE ELECTRON LEAKAGE FROM *RHODOBACTER SPHAEROIDES* BC_1 COMPLEX

Introduction

The enzymatic activity of the purified three-subunit bc_1 complex is only about 25% of that of the 4-subunit one. Several regions and individual amino acid residues on subunit IV were identified to be essential for the interaction between the subunit IV and the 3-subunit core complex in the previous chapters. However, how the subunit IV affects the activity of bc_1 complex is still not clear.

It is reported that during the electron transfer through the mitochondrial bc_1 complex, a small amount of superoxide anion is generated due to the electron leakage. Thus the amount of superoxide generated by the bc_1 complex should be correlated to how well the protein is able to prevent electron leaking. On the other hand, the loss of electrons may decrease the enzymatic activity of the bc_1 complex. It is possible that the bc_1 complex with supernumerary subunits has better control on the electron leakage and therefore has higher activity.

In this chapter, evidences of the role of subunit IV in preventing electrons from leaking out in the *R. sphaeroides* cytochrome bc_1 complex are presented and discussed.

Results and Discussion

Effect of Subunit IV on Reduction of Cytochrome *b* and Cytochrome c_1 by Ubiquinol

To study the role of subunit IV in the reduction of the bc_1 complex by ubiquinol, either oxidized 3-subunit complex or 4-subunit complex was mixed with reduced ubiquinol in a stopped-flow mixer to examine the pre-steady-state reduction of the enzyme with ubiquinol. Since the concentration of ubiquinol (25 μM) is much higher than the concentration of the bc_1 complex (3 μM) in the reaction mixture, the concentration of the ubiquinol can be considered a constant during the reaction. This allows the reaction to be analyzed as a first-order reaction. Figure 15-A, B, and C show the 1-sec time course of the reduction of cytochrome *b*, in the absence of inhibitor, in the presence of a Q_i site inhibitor antimycin A, and Q_o site inhibitor myxothiazol respectively, while Figure 15-A', B' and C' show the time courses of the reduction of cytochrome c_1 under the same conditions.

In Figure15-A, the reduction of cytochrome *b* is a "tri-phasic" reaction as reported with yeast bc_1 reduced by menoquinol (86). Such tri-phasic reaction consists of a rapid reduction phase (0-40 msec), a partial re-oxidation phase (40-100 msec), and a slow re-reduction phase (after 100 msec). Based on the Q-cycle mechanism, these 3 phases represent 1) the reduction of cytochrome *b* at the Qo site, 2) the oxidation of cytochrome *b* at the Qi site, and 3) slow reduction of cytochrome *b* and the equilibrium between

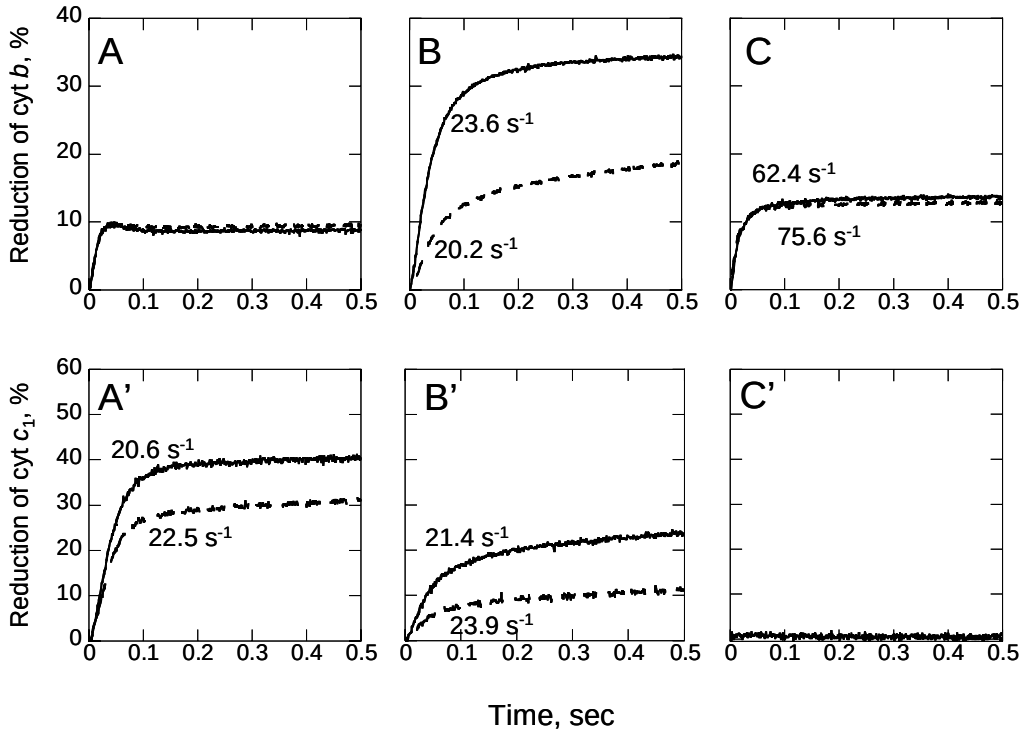

FIG 15. **Time course of reduction of cytochrome *b* and c_1 by ubiquinol in 4-subunit *R.s.* bc_1 complex (solid line) and in 3-subunit complex (dashed line) in the absence of inhibitor (A and A'), the presence of antimycin A (B and B') and in the presence of myxothiazol (C and C').** The reactions were initiated by mixing equal volume of 50 μM reduced $Q_0C_{10}Br$ in 5 mM NaH_2PO_4, 0.01% DM, 0.1% BSA, 1mM KCN, 1mM NaN_3, and 6 μM *bc*1 complex in 100 mM phosphate buffer, pH 7.4 containing 0.01% DM, 0.1% BSA, 1mM KCN and 1mM NaN_3 at 23°C in the stopped-flow mixer. Antimycin A or myxothiazol was added to 30 μM. The reduction of cytochrome *b* and c_1 was calculated from the wavelength pair of A_{561nm} -$A_{542\ nm}$ and A_{551nm} - $A_{532\ nm}$ respectively, and converted to percentage of reduction by using potassium ferric cyanide oxidized spectrum as 0 reduction and sodium dithionite reduced spectrum as 100% reduction. All traces here are the average of 3 repeated measurements. The numbers indicated beside the curves are the estimated rate constants.

reduction and oxidation. However, in Figure 15-A, the subunit IV shows little effect on the curves of cytochrome *b* in the absence of inhibitor; the traces of 3-subunit core complex and 4-subunit complex are almost identical.

Figure 15-A' displays the time course of cytochrome c_1 reduction in the absence of inhibitors. Both traces of 3-subunit and 4-subunit complex can be fitted very well with first-order-double-component equations, indicating that the reactions consist of a fast phase and a slow phase. However, the 0.5 sec time-courses are dominated by the fast phase, and the slow phase is barely noticed. For the reduction of cytochrome c_1 in the 3-subunit and 4 subunit complexes, the first-order rate constants of the fast phase are estimated as 22.5 and 20.6 s^{-1} respectively. While the rate constants do not show significant difference between these two traces, the difference lies in the extent of the reduction. At 0.5 sec after mixing, about 40% of cytochrome c_1 in the 4-subunit complex is reduced, but only 31% of the cytochrome c_1 in the 3-subunit complex is reduced.

Figure 15-B and B' show the time courses of cytochromes *b* and c_1 reduction by ubiquinol in the presence of the Q_i site inhibitor antimycin A. Since the Q_i site is blocked, reduced cytochrome *b* is not able to be oxidized at the Q_i site. Therefore, the reduction of the cytochrome *b* no longer shows the 'tri-phasic" trace as seen in Figure 15-A. In the presence of antimycin A, the reductions of both cytochromes *b* and c_1 can be fitted with first-order-double-component equations. The rate constants for the reduction of cytochrome *b* in the 3-subunit and 4 subunit complexes are 20.2 and 23.6 s^{-1} respectively; while the rate constants of the reduction of cytochrome c_1 are 23.9 and 21.4 s^{-1} respectively. No significant difference is observed between the rate constants of the 3-

subunit and 4-subunit complexes. The 4-subunit bc_1 complex has significantly more cytochrome *b* and c_1 being reduced than the 3-subunit complex after 0.5 sec of reaction.

Upon treatment of Q_o site inhibitor myxothiazol (see Figure 15-C and C'), the reductions of cytochrome *b* are also first-order double-component curves, while the cytochrome c_1 shows no reduction by ubiquinol in 0.5 sec. The cytochrome *b* is believed to be reduced by ubiquinol through the Q_i site as the Q_o site is blocked by the inhibitor (86). The fast phase rate constants of reduction of cytochrome *b* in 3-subunit complex and 4-subunit complex are 75.6 and 62.4 s^{-1} respectively, suggesting that the electron transfer through Q_i site is slightly faster in the 3-subunit complex than in the 4-subunit complex.

According to the Q-cycle mechanism, both cytochrome *b* and cytochrome c_1 are reduced by ubiquinol through Q_o site in either the native or antimycin A treated bc_1 complex. Surprisingly, little difference can be found between 3-subunit complex and 4-subunit complex on the rate constants for reduction of cytochromes *b* or c_1 through Q_o site, suggesting subunit IV does not affect the ubiquinol oxidation at the Q_o site. However, the difference in the extent of reduction of cytochromes *b* and c_1 shown on Figure 15-A', B, and B' suggests that the complex without subunit IV is losing significant amount of electron during the reaction compared to the 4-subunit complex.

Figure 16 shows the 50-sec time course of cytochrome *b* and c_1 reduction by ubiquinol in the presence of antimycin A. Cytochromes *b* of both the 3-subunit complex and the 4-subunit complex start getting oxidized at about 5 sec after mixing (see Figure 16, top panel), indicating that electrons are leaking out from cytochrome *b* (very likely b_L). Meanwhile, cytochromes c_1 continue to be slowly reduced and reach about the same

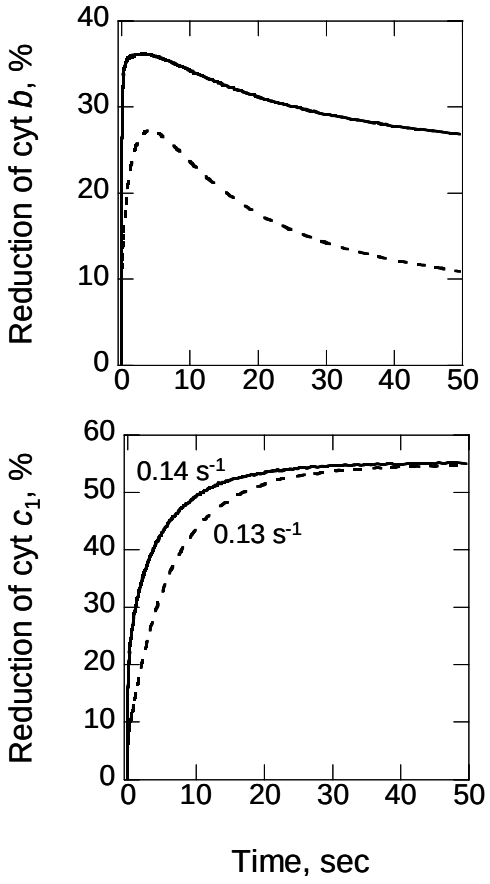

FIG 16. **Time course of reduction of cytochrome *b* and c_1 by ubiquinol in 4-subunit *R.s.* bc_1 complex (solid line) and in 3-subunit complex (dashed line) in the presence of antimycin A.** The reactions were initiated by mixing equal volume of 50 μM reduced $Q_0C_{10}Br$ in 5 mM NaH_2PO_4, 0.01% DM, 0.1% BSA, 1mM KCN, 1mM NaN_3, and 6 μM *bc*1 complex in 100 mM phosphate buffer, pH 7.4 containing 0.01% DM, 0.1% BSA, 1mM KCN and 1mM NaN_3 at 23°C in the stopped-flow mixer. Antimycin A was added to 30 μM. The reduction of cytochrome *b* and c_1 was calculated from the wavelength pair of A_{561nm} -$A_{542\ nm}$ and A_{551nm} - $A_{532\ nm}$ respectively, and converted to percentage of reduction by using potassium ferric cyanide oxidized spectrum as 0 reduction and sodium dithionite reduced spectrum as 100% reduction. All traces here are the average of 3 repeated measurements. The numbers beside curves are estimated rate constants of the slow phase.

level of reduction for both the 3-subunit and the 4-subunit complexes (see Figure 16, bottom panel), indicating that there is no difference between the two complexes in the total amount of electron being transferred into the high potential chain (ISP and cytochrome c_1). Based on the bifurcated quinol oxidation at the Q_o site, there should be no difference between the two complexes in the amount of electrons transferred into the low potential chain (cytochromes b_L and b_H). Apparently, that is not the case. Figure 16 clearly demonstrates that the 3-subunit complex loses much more electrons from its regular electron-transfer pathway than the 4-subunit complex does. Therefore, it is reasonable to assume that subunit IV is able to decrease the electron leaking from the bc_1 complex.

Effect of Subunit IV on Superoxide Generation by the bc_1 Complex

To support the hypothesis that subunit IV functions in decreasing electron leakage, superoxide generation by bc_1 complex was determined. If the hypothesis is correct, more superoxide should be generated from the 3-subunit complex than from the 4-subunit complex under the same condition. Superoxide radicals can be measured by monitoring the chemiluminescence produced by the MCLA-superoxide adduct (82,83).

To measure the generation of superoxide radicals in the pre-steady state reaction of the reduction of the bc_1 complex by ubiquinol, the stopped-flow assays were set up in the same way as the reduction kinetics assays, except that MCLA was added to the quinol containing reservoir to a final concentration of 4.0 μM. Figure 17 shows the 1-sec time courses of the superoxide radical generation during reduction of bc_1 by ubiquinol in absence of any inhibitor (A), in the presence of antimycin A (B) and myxothiazol (C). The results show that subunit IV does decrease the superoxide radical generation on the

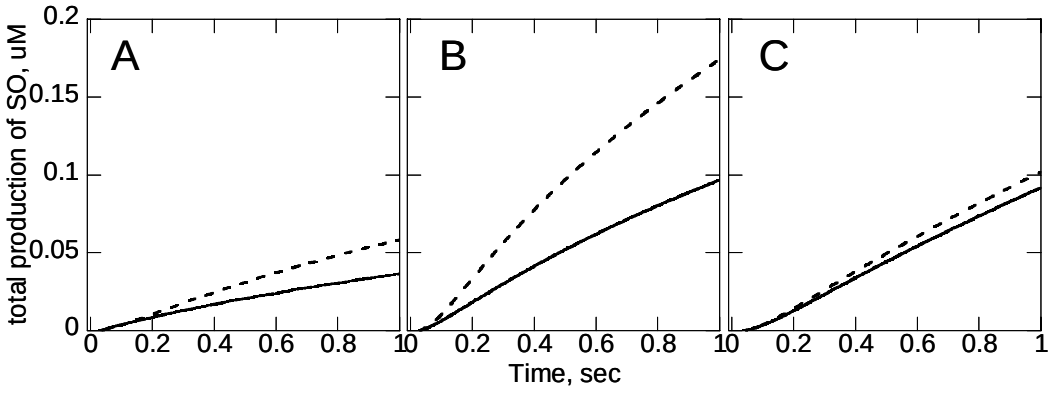

FIG. 17. **Time course of superoxide generation in 4-subunit (solid line) and in 3-subunit (dashed line) complexes in the absence of inhibitor (A), the presence of antimycin A (B) and in the presence of myxothiazol (C).** Fifty μM reduced $Q_0C_{10}Br$ in 5 mM NaH_2PO_4, 0.01% DM, 0.1% BSA, 1mM KCN, 1mM NaN_3 and 4 μM MCLA were mixed with equal volume of 6 μM bc_1 complex in 100 mM phosphate buffer, containing 0.01% DM, 0.1% BSA, 1mM KCN, and 1mM NaN_3 at 23°C by a stopped-flow mixer to initiate the reaction. Antimycin A or myxothiazol was added to 30 μM in the bc_1 complex sample where needed. The superoxide induced MCLA chemiluminescence was detected by the emission photomultiplier of the stopped-flow photometer and converted to total production of superoxide by using the superoxide generated by xanthine oxidase reaction as a standard. All traces here are the average of 6 repeated measurements.

native and antimycin A treated complex, but it has no significant effect on the myxothiazol treated complex. Clearly, this observation supports our hypothesis that subunit IV is able to decrease the electron leaking and hence the generation of superoxide.

Effect of Oxygen on the Extent of Cytochrome *b* Reduction in the bc_1 Complex

The hypothesis is further confirmed by observing the reaction kinetics of antimycin A treated complex and ubiquinol under anaerobic conditions. Figure 18 displays the time courses of the reduction of cytochrome *b* in the cytochrome bc_1 complex by ubiquinol under either aerobic (A) or anaerobic (B) condition. Due to the difficulty in obtaining the anaerobic condition in the stopped-flow mixer, the results in Figure 18 were done by manually mixing the components in an anaerobic cuvette instead of using the stopped-flow mixer. Therefore the time zero in Figure 18 is actually about 7-8 sec after mixing. Considering the delay, the time courses shown in Figure 18-A is actually the same as those done by stopped-flow mixer shown in the top panel of Figure 16. Therefore, in Figure 18-A, the 3-subunit complex shows only 26% of cytochrome *b* reduced at the beginning of the time course while the 4-subunit complex shows 36%; at the end of the time courses (80 sec), only 4% of cytochrome *b* is still reduced in the 3-subunit complex, whereas 17% of cytochrome *b* is reduced in 4-subunit complex. As discussed previously, we assume that the difference is due to the role of subunit IV in decreasing electron leaking.

The anaerobic condition for Figure 18-B was reached by several vacuuming and argon flushing cycles before the mixing. Cytochrome *c* oxidase showed less than 0.5% activity under such condition. Figure 18-B shows that the curves of the two complexes become

very similar under the anaerobic condition. In the other words, when oxygen is absent in the system, subunit IV effect on the cytochrome *b* oxidation is not observed any more.

To establish the relationship between higher superoxide generation and low activity of the 3-subunit complex, the activity of the bc_1 complex was assayed under anaerobic conditions. If the oxygen is the cause of electron leakage and the low activity of the 3-subunit complex, the activity should be higher under anaerobic conditions. However, removing oxygen was not able to increase the enzymatic activity of the 3-subunit complex. Therefore, how the electron leakage affects the bc_1 complex's activity is still under investigation.

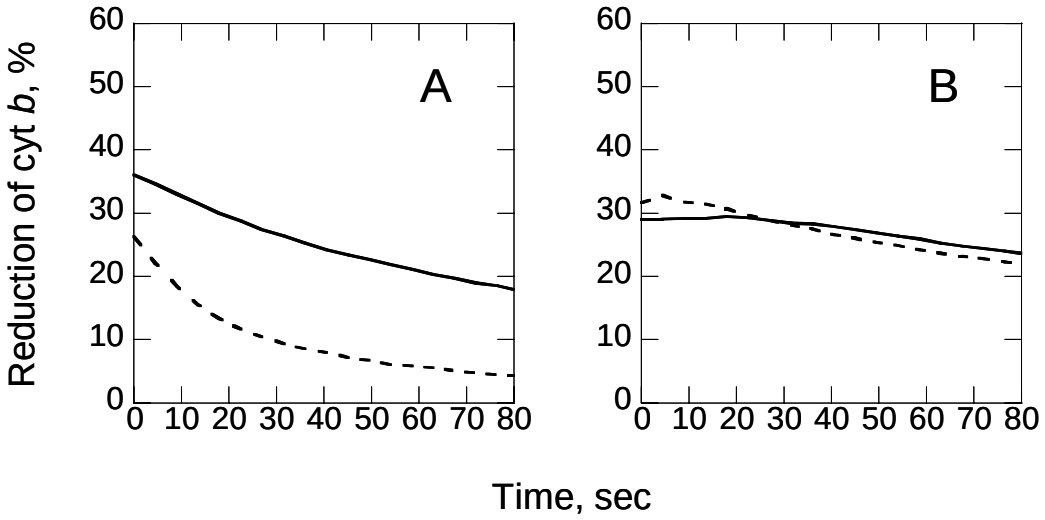

Figure 18. **The effect of oxygen on the reduction of cytochrome *b* in *R.s.* bc_1 3-subunit complex (dashed line) and 4-subunit complex (solid line) in the presence of antimycin.** The traces show the time courses of reduction of cytochrome b in the antimycin A treated complexes in either aerobic (A) or anaerobic (B) condition. The reactions were initiated by mixing 200 µl of 125 µM reduced $Q_0C_{10}Br$ from the sidearm of an anaerobic cuvett into 900 µl of 3.3 µM bc_1 complex in the main chamber of the cuvett. Anaerobic condition was reached by repeatedly evacuating and flushing with argon. $A_{560.8nm} - A_{541.6nm}$ was monitored and converted to percentage of cytochrome *b* reduction by using potassium ferric cyanide oxidized sample as 0 reduction and sodium dithionite reduced sample as 100% reduction. Due to the delay of the manual mixing, the time 0 here actually is about 7-8 second after the mixing. All traces here are the average of 3 repeated measurements.

REFERENCES

1. Hauska, G., Hurt, E., Gabellini, N., and Lockau, W. (1983) *Biochim Biophys Acta* **726**, 97-133

2. Hatefi, Y. (1985) *Annu Rev Biochem* **54**, 1015-1069

3. Trumpower, B. L. (1990) *Microbiol Rev* **54**, 101-129

4. Trumpower, B. L., and Gennis, R. B. (1994) *Annu Rev Biochem* **63**, 675-716

5. Berry, E. A., Guergova-Kuras, M., Huang, L. S., and Crofts, A. R. (2000) *Annu Rev Biochem* **69**, 1005-1075

6. Cramer, W. A., Black, M. T., Widger, W. R., and Girvin, M. E. (1987) in *The Light Reaction* (Parker, J., ed), pp. 447-493

7. Hauska, G., Nitschke, W., and Herrmann, R. G. (1988) *J Bioenerg Biomembr* **20**, 211-228

8. Trumpower, B. L. (1990) *J Biol Chem* **265**, 11409-11412

9. Chance, B. (1974) in *Dynamics of Energy-transducing Membranes* (Ernster, L., Estabrook, R. W., and Slater, E. C., ed), pp. 553-578, Elsevier Science Publishers, Amsterdam

10. Mitchell, P. (1976) *J Theor Biol* **62**, 327-367

11. Trumpower, B. L. (1976) *Biochem Biophys Res Commun* **70**, 73-80

12. Trumpower, B. L., and Edwards, C. A. (1979) *J Biol Chem* **254**, 8697-8706

13. Rieske, J. S. (1986) *J Bioenerg Biomembr* **18**, 235-257

14. Matsuno-Yagi, A., and Hatefi, Y. (1999) *J Biol Chem* **274**, 9283-9288

15. Link, T. A. (1997) *FEBS Lett* **412**, 257-264

16. Junemann, S., Heathcote, P., and Rich, P. R. (1998) *J Biol Chem* **273**, 21603-21607

17. Snyder, C. H., Gutierrez-Cirlos, E. B., and Trumpower, B. L. (2000) *J Biol Chem* **275**, 13535-13541

18. de Vries, S., Albracht, S. P., Berden, J. A., and Slater, E. C. (1981) *J Biol Chem* **256**, 11996-11998

19. Orii, Y., and Miki, T. (1997) *J Biol Chem* **272**, 17594-17604

20. Brandt, U. (1998) *Biochim Biophys Acta* **1365**, 261-268

21. Crofts, A. R., and Wang, Z. G. (1989) *Photosynthesis Research* **22**, 69-87

22. Xia, D., Yu, C. A., Kim, H., Xia, J. Z., Kachurin, A. M., Zhang, L., Yu, L., and Deisenhofer, J. (1997) *Science* **277**, 60-66

23. Iwata, S., Lee, J. W., Okada, K., Lee, J. K., Iwata, M., Rasmussen, B., Link, T. A., Ramaswamy, S., and Jap, B. K. (1998) *Science* **281**, 64-71

24. Zhang, Z., Huang, L., Shulmeister, V. M., Chi, Y. I., Kim, K. K., Hung, L. W., Crofts, A. R., Berry, E. A., and Kim, S. H. (1998) *Nature* **392**, 677-684

25. Hunte, C., Koepke, J., Lange, C., Rossmanith, T., and Michel, H. (2000) *Structure Fold Des* **8**, 669-684

26. Gao, X., Wen, X., Yu, C., Esser, L., Tso, S., Quinn, B., Zhang, L., Yu, L., and Xia, D. (2002) *Biochemistry* **41**, 11692-11702

27. Kurisu, G., Zhang, H., Smith, J. L., and Cramer, W. A. (2003) *Science* **302**, 1009-1014

28. Stroebel, D., Choquet, Y., Popot, J. L., and Picot, D. (2003) *Nature* **426**, 413-418

29. Kim, H., Xia, D., Yu, C. A., Xia, J. Z., Kachurin, A. M., Zhang, L., Yu, L., and Deisenhofer, J. (1998) *Proc Natl Acad Sci U S A* **95**, 8026-8033

30. Tian, H., Yu, L., Mather, M. W., and Yu, C. A. (1998) *J Biol Chem* **273**, 27953-27959

31. Tian, H., White, S., Yu, L., and Yu, C. A. (1999) *J Biol Chem* **274**, 7146-7152

32. Xiao, K., Yu, L., and Yu, C. A. (2000) *J Biol Chem* **275**, 38597-38604

33. Brandt, U., and von Jagow, G. (1991) *Eur J Biochem* **195**, 163-170

34. Ding, H., Moser, C. C., Robertson, D. E., Tokito, M. K., Daldal, F., and Dutton, P. L. (1995) *Biochemistry* **34**, 15979-15996

35. Yu, C. A., Tian, H., Zhang, L., Deng, K. P., Shenoy, S. K., Yu, L., Xia, D., Kim, H., and Deisenhofer, J. (1999) *J Bioenerg Biomembr* **31**, 191-199

36. Yu, C. A., Xia, D., Kim, H., Deisenhofer, J., Zhang, L., Kachurin, A. M., and Yu, L. (1998) *Biochim Biophys Acta* **1365**, 151-158

37. Xiao, K., Chandrasekaran, A., Yu, L., and Yu, C. A. (2001) *J Biol Chem* **276**, 46125-46131

38. Gutierrez-Cirlos, E. B., and Trumpower, B. L. (2002) *J Biol Chem* **277**, 1195-1202

39. Yang, X. H., and Trumpower, B. L. (1988) *J Biol Chem* **263**, 11962-11970

40. Schagger, H., Brandt, U., Gencic, S., and von Jagow, G. (1995) *Methods Enzymol* **260**, 82-96

41. Ljungdahl, P. O., Pennoyer, J. D., Robertson, D. E., and Trumpower, B. L. (1987) *Biochim Biophys Acta* **891**, 227-241

42. Yu, L., Tso, S. C., Shenoy, S. K., Quinn, B. N., and Xia, D. (1999) *J Bioenerg Biomembr* **31**, 251-257

43. Kriauciunas, A., Yu, L., Yu, C. A., Wynn, R. M., and Knaff, D. B. (1989) *Biochim Biophys Acta* **976**, 70-76

44. Robertson, D. E., Ding, H., Chelminski, P. R., Slaughter, C., Hsu, J., Moomaw, C., Tokito, M., Daldal, F., and Dutton, P. L. (1993) *Biochemistry* **32**, 1310-1317

45. Tzagoloff, A., Wu, M. A., and Crivellone, M. (1986) *J Biol Chem* **261**, 17163-17169

46. Oudshoorn, P., Van Steeg, H., Swinkels, B. W., Schoppink, P., and Grivell, L. A. (1987) *Eur J Biochem* **163**, 97-103

47. Schoppink, P. J., Hemrika, W., and Berden, J. A. (1989) *Biochim Biophys Acta* **974**, 192-201

48. Schmitt, M. E., and Trumpower, B. L. (1990) *J Biol Chem* **265**, 17005-17011

49. Maarse, A. C., De Haan, M., Schoppink, P. J., Berden, J. A., and Grivell, L. A. (1988) *Eur J Biochem* **172**, 179-184

50. Phillips, J. D., Schmitt, M. E., Brown, T. A., Beckmann, J. D., and Trumpower, B. L. (1990) *J Biol Chem* **265**, 20813-20821

51. Braun, H. P., and Schmitz, U. K. (1995) *Trends Biochem Sci* **20**, 171-175

52. Deng, K., Zhang, L., Kachurin, A. M., Yu, L., Xia, D., Kim, H., Deisenhofer, J., and Yu, C. A. (1998) *J Biol Chem* **273**, 20752-20757

53. Imhoff, J. F. (1992) in *Photosynthetic Prokaryotes* (Carr, N. H. M. a. N. G., ed), pp. 53-92, Plenum Press, New York

54. Yun, C. H., Beci, R., Crofts, A. R., Kaplan, S., and Gennis, R. B. (1990) *Eur J Biochem* **194**, 399-411

55. Usui, S., and Yu, L. (1991) *J Biol Chem* **266**, 15644-15649

56. Yu, L., Mei, Q. C., and Yu, C. A. (1984) *J Biol Chem* **259**, 5752-5760

57. Andrews, K. M., Crofts, A. R., and Gennis, R. B. (1990) *Biochemistry* **29**, 2645-2651

58. Purvis, D. J., Theiler, R., and Niederman, R. A. (1990) *J Biol Chem* **265**, 1208-1215

59. Yu, L., and Yu, C. A. (1991) *Biochemistry* **30**, 4934-4939

60. Wu, J., and Niederman, R. A. (1995) *Biochem J* **305 (Pt 3)**, 823-828

61. Chen, Y. R., Usui, S., Yu, C. A., and Yu, L. (1994) *Biochemistry* **33**, 10207-10214

62. Yu, L., and Yu, C. A. (1987) *Biochemistry* **26**, 3658-3664

63. Yu, L., Yang, F. D., and Yu, C. A. (1985) *J Biol Chem* **260**, 963-973

64. Tso, S. C., Shenoy, S. K., Quinn, B. N., and Yu, L. (2000) *J Biol Chem* **275**, 15287-15294

65. Chen, Y. R., Shenoy, S. K., Yu, C. A., and Yu, L. (1995) *J Biol Chem* **270**, 11496-11501

66. Chen, Y. R., Yu, C. A., and Yu, L. (1996) *J Biol Chem* **271**, 2057-2062

67. Boveris, A., Oshino, N., and Chance, B. (1972) *Biochem J* **128**, 617-630

68. Turrens, J. F., Alexandre, A., and Lehninger, A. L. (1985) *Arch Biochem Biophys* **237**, 408-414

69. Nohl, H., and Jordan, W. (1986) *Biochem Biophys Res Commun* **138**, 533-539

70. Turrens, J. F., and Boveris, A. (1980) *Biochem J* **191**, 421-427

71. Cadenas, E., Boveris, A., Ragan, C. I., and Stoppani, A. O. (1977) *Arch Biochem Biophys* **180**, 248-257

72. Raha, S., and Robinson, B. H. (2000) *Trends Biochem Sci* **25**, 502-508

73. Wallace, D. C. (1999) *Science* **283**, 1482-1488

74. Silber, K. R., and Sauer, R. T. (1994) *Mol Gen Genet* **242**, 237-240

75. Lowry, O. H., Rosebrough, N. J., Farr, A. L., and Randall, R. J. (1951) *J Biol Chem* **193**, 265-275

76. Bradford, M. M. (1976) *Anal Biochem* **72**, 248-254

77. Pace, C. N., Vajdos, F., Fee, L., Grimsley, G., and Gray, T. (1995) *Protein Sci* **4**, 2411-2423

78. Berden, J. A., and Slater, E. C. (1970) *Biochim Biophys Acta* **216**, 237-249

79. Yu, L., Dong, J. H., and Yu, C. A. (1986) *Biochim Biophys Acta* **852**, 203-211

80. Schagger, H., and von Jagow, G. (1987) *Anal Biochem* **166**, 368-379

81. Laemmli, U. K. (1970) *Nature* **227**, 680-685

82. Nakano, M. (1990) *Methods Enzymol* **186**, 585-591

83. Zhang, L., Yu, L., and Yu, C. A. (1998) *J Biol Chem* **273**, 33972-33976

84. Yu, L., Wei, Y. Y., Usui, S., and Yu, C. A. (1992) *J Biol Chem* **267**, 24508-24515

85. Kyte, J., and Doolittle, R. F. (1982) *J Mol Biol* **157**, 105-132

86. Snyder, C., and Trumpower, B. L. (1998) *Biochim Biophys Acta* **1365**, 125-134

Vita

Shih-Chia Tso

Candidate for the Degree of

Doctor of Philosophy

Thesis: STUDIES OF THE SUPERNUMERARY SUBUNIT OF CYTOCHROME bc_1 COMPLEX FROM *RHODOBACTER SPHAEROIDES*

Major Field: Biochemistry and Molecular Biology

Biographical:

Education: Graduated from High School of National Taiwan Normal University, Taipei, Taiwan in June 1983; received Bachelor of Science degree in Botany from National Taiwan University, Taipei, Taiwan in June 1988; received Master of Science degree in Botany from Oklahoma State University, Stillwater, Oklahoma in July 1995. Completed the requirements for the Doctor of Philosophy degree with a major in Biochemistry and Molecular Biology at Oklahoma State University in July 2004.

Experience: Employed by National Taiwan University, Department of Botany as a research assistant, 1991-1993; employed by Oklahoma State University, Department of Biochemistry and Molecular Biology as a graduate research assistant, 1996-prsent.

Publications: Chen, W.-S., **Tso, S.-C**., Huang, Y.-F., and Chen Y.-R. (1992) *Taiwania* **37,** 67-77; **Tso, S.-C.** and Chen Y.-R. (1997) *Botanical Bulletin of Academia Sinica* **38,** 245-250; Yu, L., **Tso, S.-C**., Shenoy, S. K., Quinn, B. N., and Xia, D. (1999) *J. Bioenerg. Biomembr.* **31,** 251-257; **Tso, S.-C.,** Shenoy, S. K., Quinn, B. N., and Yu, L. (2000) *J. Biol. Chem.* **275**, 15287-15294; Deng, K., Shenoy, S. K., **Tso, S.-C.,** Yu, L., and Yu, C.-A.. (2001) *J. Biol. Chem.* **276,** 6499-6505; Gao, X., Wen, X., Yu, C., Esser, L., **Tso, S.-C**., Quinn, B., Zhang, L., Yu, L., and Xia, D. (2002) *Biochemistry* **41**, 11692-11702.